nature communications

Article

https://doi.org/10.1038/s41467-026-73092-2

Large stocks of permafrost soil organic carbon and nitrogen in Arctic river deltas

Received: 18 October 2024

Accepted: 30 April 2026

Published online: 29 May 2026

Check for updates

Matthias Fuchs[1,2,3] ✉, Torsten Sachs[3,4], Loeka L. Jongejans[2,5], Jens Strauss[2], Gustaf Hugelius[6,7], Gerald V. Frost[8], Benjamin M. Jones[9], Steven V. Kokelj[10], Lars Kutzbach[11], Ingmar Nitze[2], Pier Paul Overduin[2], Juri Palmtag[6,12], Chien-Lu Ping[13], Oleg S. Pokrovsky[14,15], Elizaveta Rivkina[16], Alexandra Runge[3], Lutz Schirrmeister[2], Georg Schwamborn[17], Matthias B. Siewert[18], Claire Treat[2,19], Alexandra Veremeeva[2], Sebastian Zubrzycki[20] & Guido Grosse[2,21]

Arctic deltas are highly dynamic environments at the land-ocean interface that have acted as long-term sinks of sediment, carbon (C), and nitrogen (N). Climate impacts Arctic deltas and their upstream catchments through sea-level rise, altered river discharge, increased sediment fluxes, intensified biogeochemical cycling, and permafrost thaw. As a result, soil C and N in Arctic delta deposits are becoming more bioavailable. Here, we present a C and N inventory for Arctic delta compiled from over 1600 soil samples spanning 17 river deltas. We estimate that Arctic delta deposits store 57.5 (+9.2/−8.2) Pg C and 3.8 (+0.8/−0.7) Pg N across a combined area of nearly 100,000 km², representing large and potentially vulnerable biogeochemical pools. Our findings underscore the potentially pivotal role of Arctic deltas in the pan-Arctic carbon cycle and highlight their importance as dynamic zones of both C and N storage and release in a rapidly changing Arctic.

At the land-ocean interface, Arctic deltas with thick sediments rich in soil organic matter[1,2] are climate-sensitive landscapes that experience dynamic geomorphic conditions, affecting ecosystems and biogeochemical processes[3,4]. In contrast to lower-latitude deltas, Arctic deltas are characterized by low mean annual air temperatures, highly seasonal runoff regimes (spring freshet), frequent interaction with river ice and sea ice, and the presence of permafrost and periglacial landforms, such as ice-wedge polygons, near-surface segregated ice, frost mounds, and thermokarst lakes[5]. Permafrost stabilizes sediment, decreases channel mobility, inhibits groundwater flow, and influences

[1]Renewable and Sustainable Energy Institute, University of Colorado Boulder, Boulder, CO, USA. [2]Alfred Wegener Institute Helmholtz Centre for Polar and Marine Research, Potsdam, Germany. [3]GFZ Helmholtz Centre for Geosciences, Potsdam, Germany. [4]Institute of Geoecology, Technische Universität Braunschweig, Braunschweig, Germany. [5]Faculty of Science, Earth and Climate, Vrije Universiteit Amsterdam, Amsterdam, the Netherlands. [6]Stockholm University, Department of Physical Geography, Stockholm, Sweden. [7]Stockholm University, Bolin Centre for Climate Research, Stockholm, Sweden. [8]Alaska Biological Research, Inc., Fairbanks, AK, USA. [9]University of Alaska Fairbanks, Institute of Northern Engineering, Fairbanks, AK, USA. [10]Northwest Territories Geological Survey, Government of Northwest Territories, Yellowknife, NT, Canada. [11]Department of Earth System Sciences, University of Hamburg, Hamburg, Germany. [12]Swedish Nuclear Fuel and Waste Management Co., SKB, Solna, Sweden. [13]University of Alaska Fairbanks, Palmer Research Center, Agriculture and Forestry Experiment Station, Palmer, AK, USA. [14]Geoscience and Environment Toulouse, CNRS, University of Toulouse, Toulouse, France. [15]BIO-GEO-CLIM Laboratory, Tomsk State University, Tomsk, Russia. [16]Kovda Institute of Physicochemical, and Biological Problems in Soil Science, Russian Academy of Sciences, Pushchino, Russia. [17]Eberswalde University for Sustainable Development, Department LGW, Eberswalde, Germany. [18]Umeå University, Department of Ecology and Environmental Science, Umeå, Sweden. [19]Department of Agroecology, Center for Landscape Research in Sustainable Agricultural Futures, Aarhus University, Aarhus, Denmark. [20]Universität Hamburg, Earth and Society Research Hub, School of Integrated Climate and Earth System Sciences, Hamburg, Germany. [21]University of Potsdam, Institute of Geosciences, Potsdam, Germany. ✉e-mail: matthias.fuchs@colorado.edu

erosional processes[6,7], favoring the rapid accumulation of alluvial sediments, ground ice development, and organic matter sequestration.

Geologically, modern deltas in the Arctic began forming when the rise of the post-glacial sea level largely stabilized during the mid-Holocene[1,8,9]. Over long time scales, Arctic deltas can be characterized as sinks of organic carbon (C) and nitrogen (N), form sustained deposition of organic-rich sediments, and are considered large permafrost C pools[2,10]. However, given that the warming rates in the Arctic are two to four times greater than the global average[11–13], Arctic deltas, strongly dominated by various forms of ground ice, river and lake ice, and sea ice[1], are susceptible to major hydro-climate driven changes. Arctic deltaic environments are sensitive to multiple, often interacting changes in climate, hydrology, and disturbance regimes in both the river catchment and delta areas. For example, increasing river discharge[14–16] (associated with increased sedimentation, geochemical and C fluxes originating from thawing permafrost in river catchments[17,18], Fig. 1a, c), earlier river ice-breakup[19], riverbank erosion[20–23], channel migration[24], and the warming and thawing of permafrost[25] affect the catchment as well as the delta. At the land-ocean interface, declining sea-ice extent[26], enhanced coastal erosion[27], sea level rise[12,28,29], more intense storm activity[30], and flooding[31] all affect the biophysical environment of an Arctic delta. The net effects of these processes, including the intensity and seasonality of sediment transport and deposition, bank erosion and channel migration, ice breakup, and spring flooding, are anticipated to alter the dynamics and morphology of Arctic deltas. For example, recent modeling demonstrated that a changing sediment flux has implications on river delta morphology[32]. In combination with higher air temperatures, shifting vegetation cover and shrub expansion[33] will alter snow distribution patterns, thereby changing the surface energy balance and accelerating permafrost thaw[34]. These dynamic changes will likely change wildlife habitats and traditional land use[35]. In addition, the ongoing human activities in the Arctic may increasingly affect deltas where infrastructure for transportation, resource exploration and extraction (e.g., oil, gas, and sand), and waste containment are increasingly threatened by a warming climate[36,37]. This is of concern because deltas comprise productive and essential habitats for migratory fish, waterfowl, and mammals[38]. As such, they are a critical environment for Indigenous communities to harvest subsistence resources and foods[39,40].

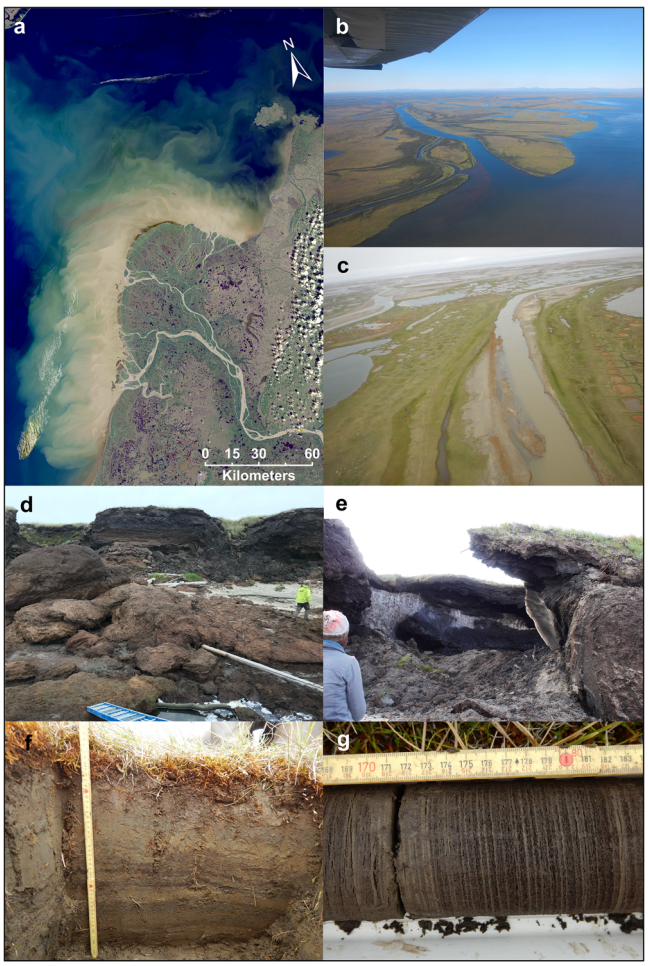

Fig. 1 | Snapshots of carbon-rich Arctic river deltas. a Massive sediment plume in front of the Yukon Delta, Landsat 8 image (bands 4, 3, 2) acquired on 6 August 2018 (Landsat-8 image courtesy of the U.S. Geological Survey[161]). **b** Low relief of the Kobuk Delta front, **c** thermokarst affected river delta and suspended sediment load in the river of the Fish Creek Delta, **d** thick, eroding peat deposits in the Lena Delta, **e** massive ice wedge on Samoylov Island, Lena Delta about 30 cm below the surface (photo credits: T. Sanders, Hereon), **f** shallow thawed, organic rich soil profile (50 cm) in the Ikpikpuk Delta, and g) carbon rich core segment from a sand bank in the Ikpikpuk Delta.

The dynamics of river deltas result in high biological productivity and a diverse distribution and deposition of sediments transported through fluvial, alluvial, wave, and tidal processes[41,42]. However, due to the extended snow- and ice-dominated winter season, these delta processes are typically inactive for up to eight months of the year. Prolonged seasonal ice coverage, in combination with permafrost conditions in soils, stabilizes delta channels and affects the morphology of Arctic deltas[7,43]. The specific hydrologic, geomorphic, and periglacial processes of Arctic deltas cause significant differences in sediment and soil organic matter accumulation, storage, and distribution compared to lower-latitude deltas (Fig. 1). For example, rapid deposition of sediments and delta surface aggradation, ecological succession, and associated syngenetic permafrost formation result in the development of ground ice and contribute to the ice-rich nature of cold region deltas[6,44,45]. The same processes enhance the sequestration and soil organic matter in permafrost. In contrast, permafrost thaw and shore erosion make formerly frozen and well-preserved ancient organic matter available for biogeochemical processing[46,47]. Therefore, permafrost dynamics driving organic matter accumulation and loss are crucial in the C and N budgets of Arctic delta deposits. There is, however, no comprehensive estimate of the volume and mass of these deposits or the amount of soil organic matter stored in Arctic deltas. Furthermore, biomass production in Arctic deltas is typically greater than that in upland tundra due to high nutrient inputs from regular flooding and sedimentation. However, rates of C accumulation and erosion, or even the stocks of organic matter components, such as C or N, have been poorly constrained with field data[10,48].

Previous studies have shown that permafrost regions store vast amounts of C and N, where peatlands, and thick deposits, such as Yedoma or Arctic deltas (up to 65 m thickness[8,49]) contribute disproportionately to this large C pool[10]. Pan-Arctic permafrost C stocks have been estimated for some thicker deposits (>3 m), such as Yedoma[50,51], thermokarst-affected areas[52], northern peatlands[53,54], and subsea permafrost[55]. However, Arctic delta permafrost carbon stocks have not been thoroughly quantified, in part because previous pan-Arctic soil carbon assessments included only minimal field data from these landscapes (from one and three Arctic deltas, respectively)[2,10]. Several recent case studies have investigated additional C and N data from individual Arctic floodplains or river deltas[56–60] offering the opportunity to update the C and N stock estimates for Arctic river deltas.

The objective of this study is to estimate the amount of soil C and N stored in Arctic delta sediment deposits. To achieve this, we provide a comprehensive high-resolution geospatial data set of pan-Arctic river deltas as well as their C and N stocks by combining the mapping of

https://doi.org/10.1038/s41467-026-73092-2

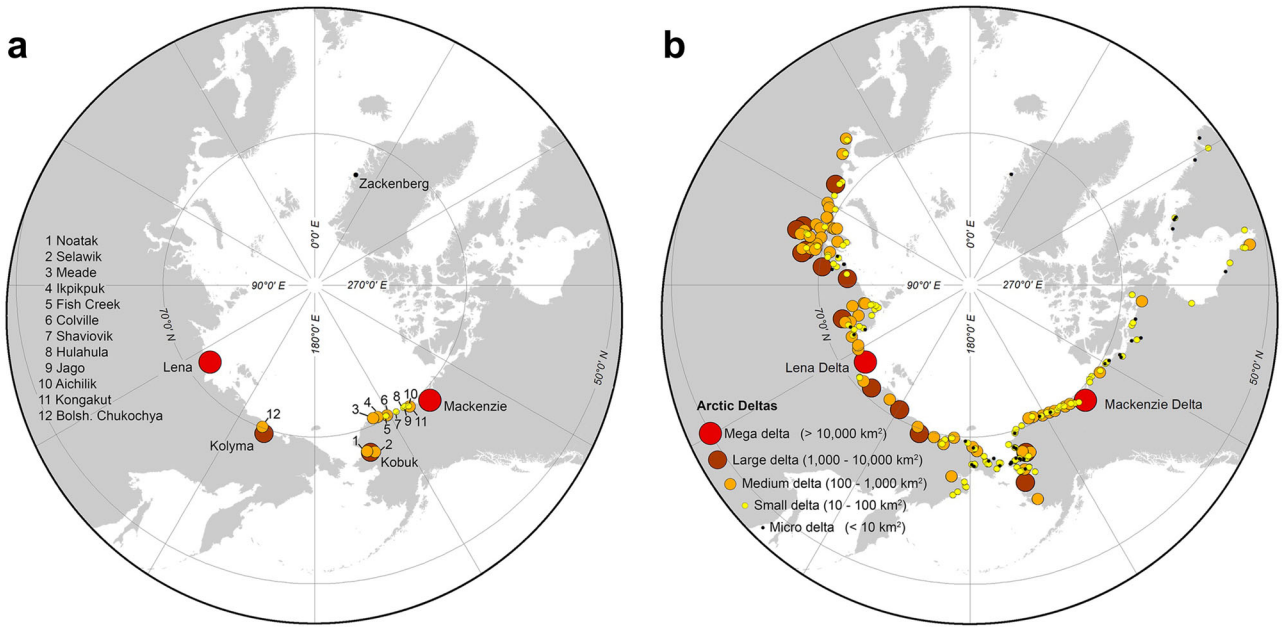

Fig. 2 | Location and size class of Arctic deltas. a 17 Arctic deltas for which we aggregated data on soil C and N in this study. More details on all 17 deltas can be found in the Supplementary Table S3.1. The dot coloration is the same as in Fig. 2b. Numbers replace names of smaller deltas. **b** All 211 mapped Arctic deltas. Deltas are divided into five different size classes from mega to micro delta. The two mega deltas (Lena and Mackenzie) are named on the map and only a subset of micro deltas is mapped (black dots). For example only one micro delta on Greenland is mapped.

delta extent, field data-based estimates of deposit thicknesses, and published and previously unpublished field and laboratory data from 156 soil cores and sea and river bank exposures collected in 17 different Arctic deltas (Fig. 2a). Through this synthesis we provide a nearly threefold (+280%) increase in the number of analyzed cores compared to previous studies. We estimate that Arctic deltas (including frozen and non-frozen deposits) store 57.5 Pg C and 3.8 Pg N, comprising about 5% and 6% of global permafrost region C and N stocks, respectively, in less than 1% of the terrestrial permafrost extent. These dynamic Arctic deltas store about 2% of the global soil C in an area comprising only 0.08% of global soils[61]. Our study initiates a much-needed improvement in the quantitative understanding of the large C and N stocks in permafrost regions and Arctic deltas, highlighting them as hotspots for C and N storage and underscoring the need for further study. Absent from current Earth System Models, these long-term C and N reservoirs are vulnerable to abrupt transitions into sources of C, N, and other nutrients, driven by enhanced overbank sedimentation, thaw-induced erosion, and shifting channel dynamics. In addition, the reduction of sea ice will allow wave energy and sea level rise to inundate and erode low-lying deltaic deposits, which will have severe impacts on these landscapes at the land-ocean interface.

Results and discussion

Arctic deltas as unique geomorphological features

We conducted a comprehensive survey of Arctic Ocean and Bering Sea coastlines and used high-resolution satellite imagery to identify and delineate 211 Arctic deltas (Fig. 2b). These deltas collectively cover an area of 98,620 km^2 and can be divided into five size classes, from micro-delta (< 10 km^2) to mega-delta (> 10,000 km^2) (Supplementary Table S1.1). However, the micro-delta class only contains a fraction of all deltas smaller than 10 km^2 (meaning that not all Arctic micro-deltas have been mapped: see methods for details). The two mega-deltas of the Lena and Mackenzie rivers account for 34% of the entire Arctic delta area and exhibit high internal heterogeneity and significant differences compared to each other (e.g., unglaciated vs. glaciated catchments, sediment delivery, and surficial geology). In contrast, small and micro-deltas are abundant (n = 142) but constitute only a minor portion of the total delta area (4%). Our inventory considered Arctic deltas in a geographic sense (e.g., location of the river mouth at the Arctic Ocean) rather than according to a definition of their morphology (e.g., a deltaic shape) or the fact that all surficial deposits are strictly fluvial in origin. This recently introduced, more comprehensive approach[1] allows a range of fluvially deposited sediments from prograding deltas, estuaries, and alluvial fans to be included. As a result, the mapped delta extents include diverse landscapes and sedimentary materials, including fluvial, eolian, proluvial, and peat deposits overlying older sedimentary deposits. Permafrost and ground ice have stabilized Arctic delta deposits[1], but permafrost thaw will weaken the bonding role of ground ice. In addition, cold climate and permafrost have diminished annual sediment delivery by Arctic rivers compared to low-latitude deltas, despite delivering 10% of global river discharge[1,62]. However, climate-driven permafrost thaw is expected to increase these fluxes[63]. Arctic deltas are important fluvial deposits, where sediment accumulation and dispersal is influenced by river ice and permafrost in the delta[1,64], and organic matter burial efficiency is high compared to low-latitude deltas[65].

Here we estimate that approximately 77% of the pan-Arctic delta area is underlain by continuous permafrost[66], 12% by discontinuous permafrost, 8% by sporadic, 2% by isolated permafrost, and 1% by no permafrost. However, considering that near-surface permafrost does not always accurately reflect the conditions at greater depth due to the shifting nature of channels, the thermal effect of water bodies, and vegetation heterogeneity[67,68], the estimates of volumetric permafrost fraction are subject to high uncertainty. Permafrost has a significant impact on the geomorphology of Arctic deltas, so thawing will have major effects on the future evolution of Arctic deltas[64]. In many Arctic deltas, particularly those with marine influence, saline permafrost and cryopeg brines—unfrozen hypersaline layers in the subsurface that persist well below 0 °C— further complicate subsurface thermal regimes and influence thaw dynamics[69]. In addition, bank erosion by migrating river channels may be one of the most rapid mechanisms for degrading permafrost and altering the shape of Arctic deltas[70–72]. However, increased vegetation growth and shrubification can reduce bank erosion and channel migration[24,73,74].

Table 1 | Soil organic C and N stocks and SV for Arctic delta deposits

	Soil organic C stock [Pg C]	N stock [Pg N]	Sediment volume [km^3]
Delta, all deposits	57.5 +9.2/−8.2	3.8 +0.8/−0.7	3519 +753/−613
Delta, non-frozen deposits	18.4 +4.4/−3.8	1.2 +0.3/−0.3	1062 +325/−260
Delta, frozen deposits	39.1 +6.7/−6.0	2.6 +0.6/−0.5	2457 +555/−456

Numbers below indicated with a +/− are the 95% confidence intervals.

The thickness of Arctic deltaic deposits has been evaluated based on deep deposit data available for five deltas (Supplementary Table S2.1). This is the only data available on Arctic delta thickness and shows the sparsity of information on Arctic deltas. This depth information was used to calculate an ordinary least square regression between delta thickness and area (R = 0.97; Supplementary Fig. S2.1), allowing for a first-order estimate of the thickness for all 211 deltas. This estimate should be treated carefully as the data basis is very sparse for Arctic delta deposit thickness. On this basis the sediment volume (SV) of all Arctic deltas was estimated to be approximately 3519 km^3 (Table 1). Of that volume, based on the permafrost distribution and general assumptions of relationships between water bodies and talik occurrence, 2457 km^3 may be regarded perennially frozen (permafrost), and 1062 km^3 may be considered seasonally or non-frozen sediment deposits. The frozen SV excludes ice-wedges, estimated to comprise 6%[75,76] of the top five meters of deltaic deposits (see methods). Besides ice-wedge content, water bodies (lakes, ponds, river channels) are a widespread landscape feature in Arctic deltas, occupying about 3% of the delta volume, and, on average, 24% of the delta area[77]. Waterbody coverage varies between <1 to 77% of the delta area, and the average water body depth is assumed to be 5 m following a prior estimate[10].

Arctic deltas contain thick C and N-rich deposits

We compiled a pan-Arctic C and N data set by synthesizing previously published data[58,60,76,78] and new or unpublished soil data from disparate locations, including the Kobuk, Selawik, and Noatak deltas in northwestern Alaska[79] and the Lena Delta in Siberia[80,81] (see Supplementary Table S3.2). Our data set comprises 156 soil (or sediment) cores (or exposures) from Arctic deltas, including 1640 individual samples (from 0 to 65 m depth). Of these samples, 1286 include N content and comprise a pan-Arctic N data set for river deltas. However, only 14% of all the samples are from depths >2 m with no non-frozen samples from >2 m depth, and only 6% of samples contain N content below 2 m depth, and therefore N estimates should be treated carefully. Since we observe a slight decrease in %C with depth (see Supplementary Fig. S3.2), we applied a depth decay model (see Supplementary Fig. S4.1) for total organic C with deposit depth to prevent overestimation of the C stocks in deep Arctic delta deposits. In addition, the SV and the soil organic C stocks were calculated for each of the delta using a Monte Carlo model simulation in the R programming language[82] (see methods). In this model, we implemented an uncertainty range for each of the input parameters (C density, area, deposit thickness, active layer depth, ice-wedge volume, water body coverage, water depth, permafrost occurrence) where for each model run a random value for each parameter is chosen from the uncertainty range. We run the model 10,000 times allowing us to calculate the mean soil organic C and soil N stocks including 95% confidence intervals (Fig. 3a, b).

Based on our compiled data set, our input variables (e.g., deposit thickness) and the 10,000 model runs, we estimate a mean total pan-Arctic C and N stock of 57.5 (+ 9.2/−8.2) (95% confidence interval) Pg C and 3.8 (+0.8/−0.7) Pg N, respectively (Fig. 3). Assuming permafrost distribution according to the most recent available map[66], deposits beneath water bodies to be unfrozen, and an average active layer depth of 0.53 m, we estimate that 68% of the C (39.1 + 6.7/−6.0 Pg C) and 70% of the N (2.6 + 0.6/−0.5 Pg N) of these stocks are currently stored in perennially frozen deposits. For our C and N stock estimates, we include all deposits in Arctic deltas, except for non-deltaic Yedoma deposits (e.g., in the Lena and Olenyok deltas) and sandy deposits on Arga Island (see Supplementary Material S8 for details), a pre-Holocene fluvial unit in the Lena Delta. If these deposits covering a total area of 8986 km^2 are included, the C and N storage in Arctic deltas increases to 63.2 Pg C and 4.2 Pg N.

The 39.1 Pg C stored in frozen Arctic delta deposits contributes 5% of the total permafrost C in the pan-Arctic permafrost region[10], despite covering only a small fraction of the total area (0.6%). Similarly, 2.6 Pg N are stored in frozen deposits, representing 4% of N in near-surface permafrost soils (67 Pg, 0–3 m[83]) and 6% of N compared to Yedoma deposits (41 Pg[84]). Other estimates of deep permafrost deposits have already been the focus of detailed studies (Table 2) (e.g., peatlands, Yedoma, and thermokarst deposits[50,52–54]) and spatially overlap with this Arctic delta estimate. However, this estimate is unique in focusing solely on Arctic delta areas.

We estimate that about 30% of the deltaic deposits are not perennially frozen. This estimate includes the seasonally frozen active layer above permafrost, unfrozen delta deposits resulting from lower (discontinuous to isolated) permafrost occurrence, and other unfrozen deltaic deposits, such as unfrozen sediments beneath water bodies and associated with saline permafrost and hypersaline brines (cryopegs) (see Supplementary Fig. S5.1). Due to the dynamic nature of shifting channels[85] and the thermal effect of water bodies, most Arctic deltas are not entirely underlain by frozen ground and contain significant volumes of unfrozen sediments in taliks (local occurrences of unfrozen deposits) and cryopegs[69]. Additionally, for deltaic regions in the continuous permafrost zone, characterized by 90–100% coverage by permafrost, we consider taliks to occur beneath water bodies or drained thermokarst lakes. As a result, on average, 63% of the surface area (including water areas) of Arctic deltas are estimated to be underlain by permafrost. However, deltas on the Arctic marginal seas (e.g., Bering Sea, Barents Sea), such as the Yukon Delta, largely lack permafrost on the active floodplain, and permafrost is likely only present on old, abandoned floodplain deposits that are no longer regularly flooded[86,87]. These (lower latitude) delta regions contribute to the large amount of C stored in unfrozen deposits and the deltas further north (70–75°N) also store a substantial amount of C in unfrozen alluvium beneath water bodies (deep channels and lakes), which results in about one-quarter of C stored in non-frozen deposits for these high-latitude deltas (see Supplementary Fig. S6.1).

Lower carbon densities but higher storage potential in Arctic deltas

We found that the average C and N densities of Arctic deltas are low compared to other landforms with thick permafrost deposits. On average, Arctic delta deposits store 16.7 kg C m^{-3}, which is more than 40% lower than C density in landscapes that are potentially affected by thermokarst (estimated to 30 kg C m^{-3})[52]. We estimated an average N density of 1.1 kg N m^{-3}, which is similar to a previous estimate[83] for non-cryoturbated mineral permafrost soils (Orthels) down to 3 m (estimated to 1.5 kg N m^{-3}). Despite the lower mean C density, Arctic deltas store a high C stock by area due to their large deposit thickness. While Arctic deltas cover smaller areas and store less bulk C than landscapes susceptible to thermokarst and peatlands, delta deposits have one of the highest C storage per area unit (583 kg C m^{-2}) due to their greater deposit thickness (average of 35 m) (Table 2).

Table 2 | C and N stocks in thick permafrost deposits

Deposits	Area [10^3 km^2]	Total soil organic C stock [Pg]	Average soil organic C stock [kg C m^{-2}]	Average soil organic C density [kg C m^{-3}]	Total N stock [Pg]	Average N stock [kg N m^{-2}]	Average N density [kg N m^{-3}]	Reference
Thermokarst deposits (0–3 m)	3640	333	91	30.3	-	-	-	Olefeldt et al.[52]
Thermokarst deposits in Yedoma region (0–6 m)	775/ 1460[a]	128 (32–227)	165	31	15 (13–17)	11	2.2	Strauss et al.[50,84]
Yedoma deposits (0–20 m)	416/ 480[a]	83 (26–144)	200	10	7 (6–8)	14	0.9	Strauss et al.[50,84]
Northern peatlands (>23°N) (0–10 m)	3700	415 (265–575)	115	46	10 (3–17)	3	4	Hugelius et al.[54]
Subsea permafrost (0–1117 m)	2500	2822 (1518–4982)	1129	3.9[b]	-	-	-	Miesner et al.[55]
Arctic deltas (0–35 m)	98	57 (49–67)	583	16.7	3.8 (3–5)	39	1.1	This study

[a]Different areas for the C and N pools: first number is for the C assessment[50], second number is for the N assessment[84].
[b]Calculated with mean depth for subsea permafrost deposits (287 m) retrieved from ref. 162.
Note: There is spatial overlap between these regional estimates, so they cannot simply be added. Numbers in brackets show the uncertainty range.

This large C and N stock per area unit suggests that processes related to abrupt permafrost thaw could have major impacts on C and N mobilization[88]. Riverbed and shore erosion[71,89,90] as well as thermokarst processes, may affect deposits at depth, through thaw and sediment mobilization, with the potential to expose large quantities of C and N to mobilization, degradation, and microbial decomposition. These processes, which can result in a more rapid and deeper thaw of permafrost substrate, occur in addition to the gradual top-down permafrost thaw, accelerated by increasing air temperatures and inundation caused by sea level rise. The thaw and degradation rates of deltaic deposits are variable due to the wide range of mechanisms. For example, erosion rates from 1 to 4 m/yr for delta riverbanks have been reported for the Colville Delta[70,71]. Although, the availability of thawed soil C and N from delta deposits for microbial turnover and release as greenhouse gases requires further investigation, intitial studies show that the degradability of active floodplain C is similar to that of other permafrost region soils[91,92] and that CH_4 production increases and becomes more substantial in a warming, wet deltaic environment[93,94]. Another study showed that alluvial soil organic matter tends to be more labile than organic matter from peatland or Yedoma deposits, highlighting the importance of deltaic, alluvial C[95].

Improving pan-Arctic delta C and N estimates

Here, we synthesized an extensive data set focusing on total soil organic C and N stocks in Arctic deltas. We lowered the total C stock estimates for Arctic deltas by about 40% compared to two previous estimates that were based on data from only three deltas[2,10] (see Supplementary Table S9.1). Our improved approach reduced the estimated thickness of delta deposits (mean weighted average of 35 m vs. >50 m). Combined with lower total organic C contents, this leads, on average, to a lower total C stock for Arctic deltas than previous studies. Despite the relative importance of Arctic deltas, they have been the least investigated type of deep permafrost C pools so far, even though they are of dynamic nature and have the ability to sequester organic matter and sediments. The large, synthesized data set in our study, which increased the number of cores by over one hundred (+280%), also included an uncertainty estimate for other parameters (deposit thickness, active layer depth, ice-wedge volume, area) for better constraining the uncertainty in the total C stock estimates in Arctic deltas. This compilation also yielded an estimate of N stocks in Arctic deltas – a metric that had not been previously assessed. We demonstrated that deltas store a significant amount of C (57.5 Pg) and N (3.8 Pg), indicating that a better understanding of biogeochemical and geomorphological dynamics is required, along with their inclusion in global soil C and N pool estimates.

This data set of 1640 samples, largely from the top 3 m of alluvial deposits, indicates a broad range of C and N as well as bulk density. In particular, the samples within the top two meters of soil show high variability in delta deposits (see Supplementary Fig. S3.1 and S3.2), which reflects alluvial succession and the burial of organic matter in different soil layers and under diverse sediment accumulation regimes (fluvial, alluvial, eolian) occurring in river deltas. These surface layers have a large spread of C and N as well as C/N ratios, which do not show a uniform distribution and point to different organic matter accumulation, transport, and decomposition processes leading to a heterogeneous soil environment. In future studies, high-resolution surface feature and vegetation mapping could be used to explore relationships with existing data on vegetation, ground-ice, and near-surface sediments[6,44,96,97], providing further insight on the variation in near-surface, C, and N characteristics. Furthermore, more sample material from deeper deposits from both, non-frozen and frozen deposits is needed to better assess the stratigraphic heterogeneity of C and N stores thereby accurately assessing stocks for deep deposits. This is particularly true for N, where only 91 samples containing N values are available for depths >2 m leading to a coarse N stock estimate that should be treated carefully.

There are, in general, only a few studies on C and N stocks in river deltas, and comparisons to low-latitude deltaic C stocks are difficult because often only the uppermost layers (<1 m) were investigated for C storage of deltaic deposits (e.g. Nile River Delta[98] or Yellow River Delta[99]). Comparable coastal-interface environments may also include tidal wetlands. A nationwide estimate of C stocks for tidal wetlands in the United States resulted in a mean C content of 27 kg C m^{-3} and a total stock of 0.72 Pg C (26,700 km^2) for the top 0-1 m of soil[100]. An estimate for all wetlands in the conterminous United States totaled 11.52 Pg C for the upper 1.2 m over a total area of 384,000 km^2 [101], an area almost four times greater than all the Arctic deltas combined. A recent study compiled soil organic C data for global tidal marshes[102], although for the top meter of deposits only, and found an average C storage of 23.1 kg C m^{-2} (0-1 m), which is very similar to the estimate of this study (21.6 kg C m^{-2} 0-1 m). Tidal marshes are estimated to occupy an area of 52,880 km^2 and store globally 1.22 ± 0.20 Pg C in the top meter of deposits[103]. That study, however, largely excluded areas from northern high latitudes, and our analysis shows that Arctic deltas could contribute 2 Pg C in the top meter of soil alone (see Supplementary Fig. S6.2). These comparisons indicate the disproportionately high importance of thick, thaw-vulnerable C

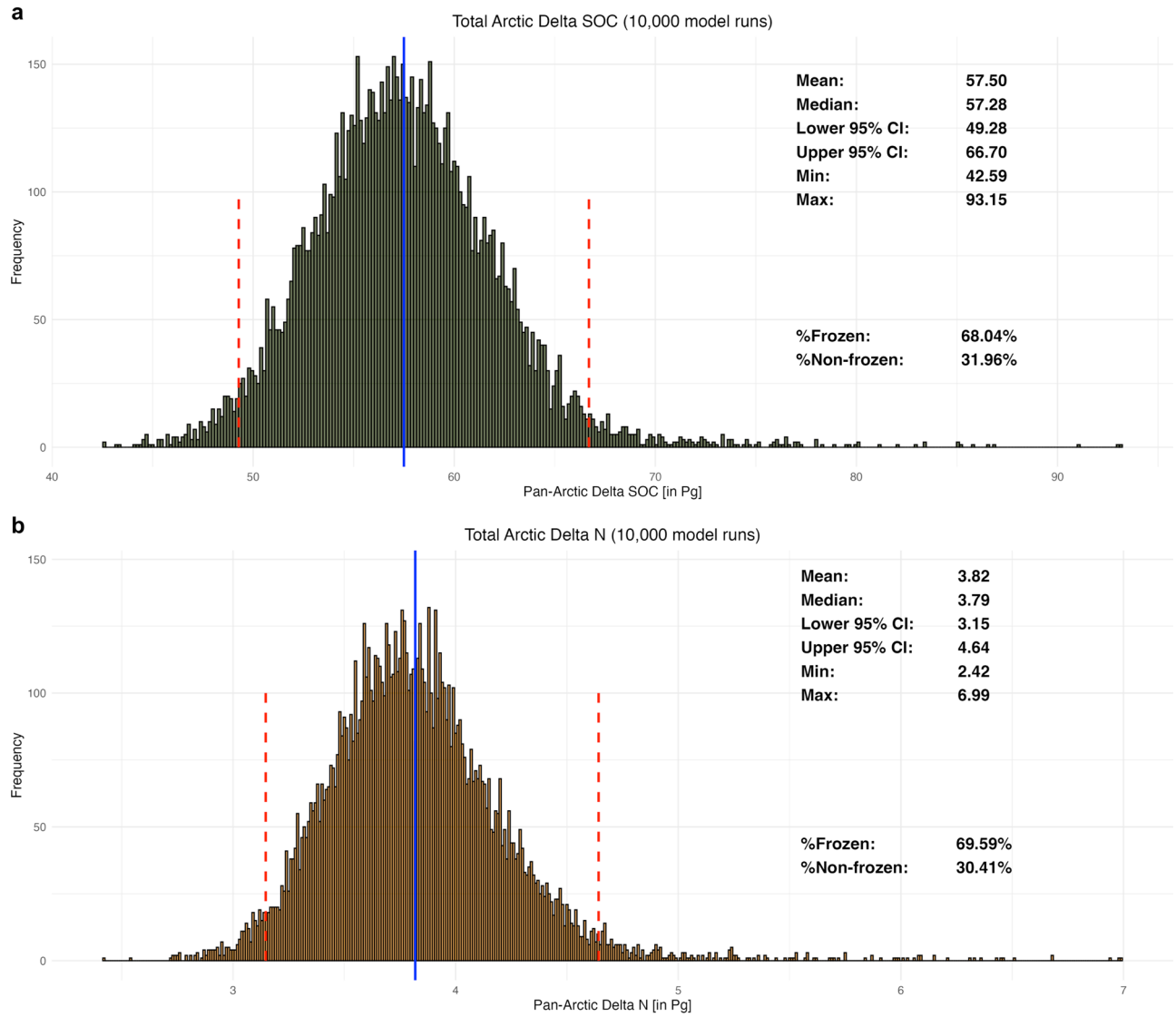

Fig. 3 | C and N stocks resulting from 10,000 model runs. a Total soil organic C (SOC) stocks for Arctic river deltas based on 10,000 model runs. **b** Soil N stocks for Arctic deltas based on 10,000 model runs. Blue line shows the mean and red dashed lines show the 95% confidence intervals.

stocks in permafrost-dominated Arctic deltas for global wetlands, requiring a better understanding of climate change impacts on Arctic deltas and the consequences of thaw for deltaic C and N mobilization.

Despite the significant increase in the number of available soil cores from Arctic deltas, there remains considerable uncertainty in our estimates for several reasons. There is still no soil data available for the majority of Arctic deltas, leaving a larger uncertainty for deltas where we have only information on the size of the delta and the fraction of surface water (92% of deltas). Notably, delta deposit thickness has been quantified for only five Arctic deltas to date. Local and regional variability in geomorphic or regional geologic setting is not accounted for in our depth estimates. Deposit thickness estimates could likely be improved with additional information for small and medium scale deltas such as sedimentation and erosion rates, or sediment loads in rivers for a more elaborated model of depths in Arctic deltas (e.g., source[104]), although various deltas might be fundamentally different on how geomorphic dynamics form and erode the deposits. Nevertheless, for most deltas such data are still lacking. Our sensitivity analysis further showed that more than 60% of the uncertainty in our results is caused by the uncertainty in deposit thickness (see Supplementary Table S7.2).

However, this study is an attempt to estimate C and N stocks for these remote areas. In addition, we used a very general understanding of "delta", meaning we do not restrict the delta term to prograding deltas but include estuaries and alluvial fans. Also, we do not have a separate estimation for taliks or cryopegs in our upscaling (in contrast to e.g. source[50]) since no C or N data are available from these unfrozen delta deposits. Nevertheless, taliks and cryopegs can be widespread in deltas (under channels and lakes or due to channel migration)[69,105] and while not all taliks are through-taliks (penetrating the entire permafrost layer), taliks can extend into the adjacent sediment[106], or persist in abandoned channels[69], which makes the estimation of non-frozen deposits challenging. Therefore, we considered all sediment deposits under water bodies as non-frozen (see Supplementary Fig. S5.1), which might lead to a slight overestimation of non-frozen deposits and therefore likely overestimates C and N stocks in non-frozen deltaic deposits. In addition, we account for non-frozen deposits by assuming a mean permafrost occurrence for each permafrost class (for example 70% permafrost occurrence in the discontinuous (50-90%) permafrost zone). We consider our approach to estimating total C and N stocks for Arctic deltas as conservative as we only include the sub-aerial topset portion of river deltas. In reality, delta deposits extend further into the near-shore zone with an extensive subaqueous foreset portion[107,108].

These subaqueous parts of Arctic deltas are poorly known but likely often feature permafrost, as bottom fast ice in these very shallow water areas allows winter frost penetration into the ground.

Arctic deltas as hot spots of change

Arctic deltas may become a significant source of C in the future, as approximately 68% of C (39.1 Pg) in Arctic deltas is stored in permafrost, which is vulnerable to thawing under a warming climate. This is similar to deposits in the Yedoma domain, where about 69% of C is stored in permafrost deposits[109] and comparable to the overall C stock in the Northern circumpolar region, where 63% (822 Pg) are stored in perennially frozen deposits[10]. In northen peatlands about 45% of C are stored in permafrost affected terrain[54]. Furthermore, permafrost-affected deltas can be ice-rich. For example, ice-wedges may add large volumes (6% in the top 5 meter of soil) of near-surface ground ice at the landscape scale[75,76,110–112], and segregated ground ice commonly develops in alluvial permafrost environments[44,113,114]. We found that most samples in our study (93%) contained excess ground ice.

Rapid thaw of permafrost with excess ice triggers thermokarst[88,115], coastal and river bank thermo-erosion[71,89,116], and enhanced lake connectivity[117], all processes that can mobilize previously permafrost-stored C and N. At the interface that links terrestrial and marine ecosystems, Arctic deltas are vulnerable to changes in sea level rise, acceleration of coastal processes and broadscale changes to the catchments. Observed declines in sea ice and river ice can lead to increased erosion. Two of the southernmost Arctic deltas—the Yukon and Kuskokwim deltas in North America—have experienced a dramatic reduction in marine sea-ice extent in recent years[118,119], which may foretell changes to other deltas as Arctic sea ice continues its rapid decline. Additionally, a rapidly rising sea level can permanently inundate large areas of these delta plains leading to increased overbank sedimentation rates. Arctic deltas further become more prone to storm floods with increasing storm frequency, higher sea levels, and longer ice-free seasons of the Arctic Ocean, causing salt-kill of tundra vegetation through salt incursion, die-off of protective vegetation layers, and subsequent degradation of permafrost[30,39,120,121] that could increase the availability of soil C and N and change Arctic deltas from C and N sinks into sources.

However, Arctic deltas could also remain (or become increased) C sinks in future. For example, deep sediments and organic matter mobilized along rivers are partially deposited and buried in deltas, effectively reducing the release of organic C from the vast northern river basins to the Arctic Ocean. Also, increased Arctic river runoff, thermokarst, and thaw of permafrost sediments upstream of river deltas enhance sediment delivery[18,22,122], potentially leading to the infilling of delta lakes[18] and likely greater overbank sedimentation that could counterbalance effects of sea level rise. All these processes can increase the sediment and C sink capacity of deltas, and the magnitude and time scale of these processes determine whether delta deposits can keep up with sea level rise and subsidence caused by permafrost thaw. Also, Arctic warming could increase the abundance and stature of vegetation in Arctic deltas[123], changing the surface energy balance[124] and likely increasing above-ground biomass, although this is probably a smaller factor in the C sink potential compared to increased sediment input from catchments and likely cannot offset C losses in the catchment[125]. Yet, an increased shrub coverage could also be an indication for thawing permafrost and changing discharge regimes in Arctic rivers[126], such as an increased winter discharge[15,127]. However, increased shrubification can potentially mitigate the destabilization of banks arising from permafrost thaw[24,73].

Hence, the future trajectory of Arctic deltas and whether deltas remain sinks or turn into C and N sources in a warming Arctic remains unknown. Which processes affecting delta C and N pools will dominate in a changing Arctic? Will increased thaw of permafrost and degradation of delta deposits lead to the release of C and N? Or will increased fluvial runoff from permafrost thaw in river catchments,[14,128–133] (with potentially higher sediment discharge), facilitate delta aggradation and burial of more C and N in delta deposits in the future despite projected sea level rise? A recent modeling study projected that more than 85% of low latitude delta loss will be driven by sea-level rise leading to a loss of 5% of the global delta area in this century[134]. Thus, understanding the future trajectory of Arctic deltas requires 1) considering the location of deltas at the land-ocean interface, and 2) recognizing that Arctic deltas are affected by both processes in the catchment and changes in the Arctic Ocean.

In this study, we created a circumarctic map of delta extents and compiled a large soil core dataset to establish a comprehensive inventory of significant C and N stocks in Arctic deltas. Our synthesis and analysis highlights the nature and magnitude of C and N stores in these globally significant depositional environments with stocks being disproportionally high relative to the area they occupy. Inventories such as ours are a crucial initial step in evaluating biogeochemical and geomorphic changes for these rapidly changing landforms at the land-water interface. With that, we provide a baseline to better understand if deltas in a warming Arctic may be affected in their capacity as carbon sinks and whether the thaw-related release of previously mostly permafrost-sequestered C and N turns Arctic deltas into a net carbon source.

Methods

In the most simplistic way to calculate C and N stocks for sediment deposits, the SV and the C density (or N density) need to be known (Eq. 1). However, in order to calculate the SV for frozen and non-frozen soils in Arctic river delta deposits, multiple additional parameters are necessary (Eqs. 2 and 3). We list (Table 3) and explain all the input parameters in the following:

$$\text{Soil organic C[kg C]} = \text{SV}[\text{m}^3]\text{xC density}[\text{kgCm}^{-3}] \tag{1}$$

$$\text{SV}_{\text{Frozen}}[\text{km}^3] = \text{A}[\text{km}^2]\text{xPF}[\%]\text{xD}[\text{m}] - \text{IW}[\%] - \text{AL}_{\text{VOL}}[\text{m}^3] - (\text{WA}[\text{m}^2]\text{x}\text{W}_{\text{Depth}}[\text{m}]\text{xPF}[\%]) \tag{2}$$

$$\text{SV}_{\text{Non-frozen}}[\text{km}^3] = \text{A}[\text{km}^2]\text{x}(1-\text{PF}[\%])\text{xD}[\text{m}] + \text{AL}_{\text{VOL}}[\text{m}^3] - (\text{WA}[\text{m}^2]\text{x}\text{W}_{\text{Depth}}[\text{m}]\text{x}(1-\text{PF}[\%])) \tag{3}$$

Area of Arctic deltas

We digitized all Arctic deltas based on (very) high-resolution images at a mapping scale of 1:5000 to 1:15,000 depending on the available Google Earth images. The area of the resulting polygon shapefile was calculated using ArcMap 10.6.1 (ESRI, Redlands, CA, USA) in North Pole Lambert Azimuthal Equal Area projection. The centroids of the polygons were calculated and used for the coordinates of the deltas. In total, we mapped 211 Arctic deltas covering a total area of 98,620 km^2 (not including Arga Island of the Lena Delta or Yedoma deposits, which were accounted for separately), and we classified the deltas into different size classes (micro to mega delta, Supplementary Table S1.1).

This simple mapping provided a first-order estimate of the total area covered by Arctic deltas. In our approach, we used a definition of 'Arctic delta' that includes typical prograding deltas but also estuaries and alluvial fans ending in the Arctic Ocean as well as inland deltas in the Arctic region. This includes deltas of size >10 km^2 and a representative subset of micro deltas (<10 km^2). Even though there are several (~100) micro deltas not covered by this data set (especially in Greenland, the Canadian Archipelago, or Novaya Zemlya Island), this only negligibly affects the final stock estimated as the 41 mapped micro deltas only contribute 0.2% of the total delta area in the Arctic

Table 3 | Input parameters for calculating the SV and upscaling of C and N stocks in Arctic deltas, including associated uncertainties

Input variable	Value used for upscaling	Uncertainty range		Source, remark
		Upper	Lower	
Area (A)	Varies for each delta $0.49 \le x \le 20{,}271\ km^2$	+14.0%	−6.8%	Mapping, this study
Active layer depth (AL_{DEPTH})	0.53 m	+0.04 m	−0.04 m	Data set, this study
Deposit thickness (D)	Varies for each delta $5 \le x \le 65$ m	+17.4 m	−17.4 m	See Supplementary Fig. S2.1
Permafrost (PF) occurrence	Varies for each delta $0 \le x \le 95\%$	+5% to +20%	−5% to −20%	Obu et al.[66]
Ice-wedge volume (IW)	5.93%	+3%	−3%	Kanevsky et al.[75] Ping et al.[76]
Water depth (W_{DEPTH})	5 m[a]	+2.5 m	−2.5 m	Included ±50% as uncertainty
Water area (WA)	Varies for each delta $0 \le x \le 77\%$	+4.6%[b]	−14.1%[b]	Pekel et al.[77]

[a]No field data is included for this estimate. Estimate is based on source[10] and an uncertainty of ±50% was included in the calculation.
[b]Average uncertainty for the water area. This varies for each delta.

(Supplementary Table S1.1). We set the beginning of a delta as the point where the river channels start to split into multiple separate channels spreading water and sediment freight across a deltaic fan or estuarine plan and develop a distinct fan ('common apex'[45], see Supplementary Fig. S1.1). Digitized Arctic deltas, therefore, include not only deltaic, fluvial deposits in a strict sedimentological definition but are based on a geographic definition of deltas. This broad definition of deltas is a necessary simplification for the upscaling based on limited data available from Arctic deltas. The digitized deltas were exported as kmz and converted into a shapefile with ArcGIS 10.6.1.

In order to have an estimate for the accuracy of the digitization, we randomly chose 20 deltas and digitized them a second time. We then compared the areas and calculated the deviations (in percentage) from the original digitization, which served as an uncertainty estimate for our digitalization approach (see Table 3) resulting in an average error of +3.6% (±10.4% standard deviation).

We used the resulting polygon layers from the mapping to clip individual Arctic deltas from the global high-resolution (30 m) Landsat-based water mask (version: 1.0 1984–2015, layer: occurrence)[77]. This allowed us to calculate the total subaerial extent (topset) of the deltas, including the spatial extent of water bodies for each delta within the subaerial extent, while we did not include the subaqueous part of deltas (foreset) for the SV calculations that accumulates in the near-shore zone. We are aware that this approach excludes a large near-shore area that contains deltaic sediments and potentially complex biogeochemical and permafrost conditions in this near-shore shallow submarine environment, however, we do neither have any information on the size of the subaqueous part of Arctic deltas nor any core data from these areas.

Thickness of delta deposits

The thickness of deposits is an important factor when assessing the SV for Arctic delta deposits. Unfortunately, thickness information from only five different Arctic deltas is available. We included information on the thickness from eight studies[2,8,49,59,135–138] (see Supplementary Table S2.1). The thickness information ranged from 7 m in micro deltas[138] to 65 m in mega deltas[8,139]. To account for the different sizes of the deltas, we used the range of 7-65 m and related it to the spatial extent of the deltas, assuming a correlation between depositional thickness and delta area. With the data from these five deltas, we extrapolated the thickness for the other deltas based on a ordinary least square linear regression, which provided the best statistical fit (Supplementary Fig. S2.1). The parameters (slope and intercept) for this ordinary least square fit were extracted together with standard errors and their 95% confidence intervals. To account for the uncertainty, we generated 1000 realistic slope-intercept pairs from a normal distribution defined by their uncertainty range keeping their covariance intact. These parameter pairs then served as input to estimate delta thickness in the soil organic C stock calculation (see below) and account for the uncertainty in thickness estimates based on the size of the delta.

Relating deposit thickness to the size of the delta is a simplification but showed a good correlation even for lower latitude deltas (see Supplementary Fig. S2.2) based on the assumption that larger deltas have a higher sediment load and, therefore, also a greater thickness of deposits. While we are aware of the few data points included, the regression provides an approximation of the thickness of deposits for the Arctic deltas included in this study. However, it becomes clear, that more data on Arctic delta deposit thickness is needed to improve the estimation and its validity.

Water bodies

The percentage of water bodies (lakes, ponds, river channels) for each delta is calculated based on a global surface water layer[77] and includes areas that are covered by water for more than 90% of the time of the ice-free season with an associated uncertainty range spanning between 85% and 95% water coverage of the ice-free season. Since we do not have data on water depth, we chose 5 m as mean water depth (as previously done in C stock estimates for Arctic deltas[10]) and included an uncertainty of ± 50%. In addition, we assumed all deposits below water bodies to be non-frozen in order to avoid overestimation of frozen deposits, since deep water bodies likely have a talik underneath.

Active layer

We assumed an average depth of 0.53 ± 0.04 m for the active layer based on our soil core data set, where 109 soil cores included a measurement of the active layer thickness.

Ice wedge volume

For frozen deposits, an ice-wedge volume of 6 ± 3 % was included in the calculations based on published data[75,76] estimating the ice-wedge volume for delta and tidal flats along the Beaufort Sea Coast in Northern Alaska. We included ice-wedge volume only for the top 5 m of deposits, since reports on ice-wedges in deltas only show an occurrence down to a depth of 5 m[71,111,140] and so far no data are available on the existence of deep delta ice-wedges. Although dissolved organic C (DOC) has been found in ice-wedges[141], the amounts of C and N storage

in ice-wedges are very minor, and therefore, considered negligible in this study.

We are aware that there might be a higher variability in ice-wedge volume and delta deposits could contain significantly more than only 6% of ice-wedge volume. However, we did a sensitivity analysis that showed that ice-wedge volume has a very small impact on the final results (Supplementary Table S7.1). Our test showed that if ice-wedge volume would decrease by 25%, this would only affect the final soil organic C stock by +0.4%.

Permafrost occurrence

The permafrost distribution within each delta was calculated based on the most recent map[66] by overlaying the permafrost distribution layer with the mapped delta land areas in a GIS analysis. For each delta we calculated the percentage coverage of continuous, discontinuous, sporadic, and isolated permafrost. With this simplified approach, permafrost presence in the terrain (according to the permafrost map[66]) assumes the entire underlying deltaic deposit to be within permafrost. However, frozen deposits in Arctic deltas are highly heterogeneous with thickness[67,68,142,143]. Therefore, in order to not overestimate the permafrost distribution, we used the average values for each permafrost class (95% for continuous, 70% for discontinuous, 30% for sporadic, and 5% for isolated permafrost), meaning that, e.g., all areas that were classified continuous were assigned 95% of permafrost. In addition, we assumed water bodies to be 5 m deep (in accordance with previous studies[10]) and therefore the deposits below water bodies were considered taliks and free of permafrost.

C and N data

For the C and N stock estimate, we synthesized soil core data from river deltas around the Arctic (Supplementary Table S3.1). Our data set includes previously published data (113 cores, 72%) as along with numerous soil data collected from additional river deltas (43 cores, 28%). In total, soil C data from 156 different locations in deltas across the Arctic were included. There was less information available on soil N, totaling 112 cores with information on N contents. For this study, twenty-five soil cores were collected from three northwestern Alaskan deltas (Kobuk, Noatak and Selawik deltas) using a 2-inch (5.08 cm) diameter SIPRE corer in August 2016. In addition, one exposure from the first Lena Delta terrace was sampled in August 2014 with a hand drill. We synthesized data sets with soil biogeochemical information from 14 deltas from the scientific literature[2,49,57,60,76,78].

For the majority of the soil cores, raw laboratory data such as total organic C content (n = 1639) and total N content (n = 1286), as well as bulk density (n = 1335) were available. The data set includes 1640 samples, of which 99% contained total organic C values, 78% contained total N values, 65% contained ice content values, and 81% contained bulk density values. Most of this data are from the top 2 m of deposits as only a few exposures and cores deeper than 2 m are available from Arctic delta deposits. This is particular true for non-frozen deposits, where no non-frozen samples are available for depths below two meters. In addition, no deep soil core information is available from the Mackenzie Delta or the Yukon Delta, and for the majority of Russian deltas no soil information is available. Assuming a slight decrease of C with depth (see Supplementary Fig. S3.2) we applied a depth-decay model (see below) for estimating our C and N stocks in order to not overestimate deep carbon stocks. In addition, our dataset consists of frozen and non-frozen samples that show a high variability within and among Arctic deltas (see Supplementary Fig. S3.3 and S3.4). Therefore, we separated the frozen and non-frozen samples in calculating the mean C and N density for the top two meters, however since there are no non-frozen samples available for depths >2 m, the depth decay model includes only frozen samples (see below).

Soil organic C and N density and stocks

Since there is a slight decrease of %C with depth (see Supplementary Fig. S3.2), we applied a depth decay model on our data for estimating % C and C density with greater depths to avoid overestimation of C and N stocks. For this depth decay, we used all the samples below 2 m depth and calculated the decay based on an exponential function (Supplementary Fig. S4.1). We excluded all the samples above 2 m depth for this model in order to not mix highly variable upper layer soils and more consistently trending lower layer soils. The depth decay model therefore includes only frozen samples, since there are no non-frozen samples available from soil layers >2 m depth. However, in the topsoil layers (30 cm increments; <2 m depth), where we have abundant samples in both classes (frozen and non-frozen) we only found statistically significantly different TOC for non-frozen and frozen samples for 60-90 cm and 90-120 cm depth increments with higher TOC values for frozen samples. In all other depth increments, we did not find a statistically significant difference in TOC between non-frozen and frozen samples in our data set (Supplementary Table S3.2).

In a next step, we extracted the TOC values for each 1 m depth increment from the depth decay model. This value was then used to estimate the dry bulk density (DBD) for each depth increment. The DBD estimation was based on the relationship of the 1335 DBD samples with TOC. This allowed us in a final step to calculate the C density [kg C m^{-3}] including a 95% confidence interval for each 1 m depth increment. The output from the depth decay model and the calculation of the C density served then as input for the total soil organic C stock calculation (see below). This means that for both frozen and non-frozen deposits below 2 m depth, the C density input is based on the depth decay model that only includes frozen samples.

For the top two meters, we split the data in four groups, non-frozen samples from 0 to 1 m, non-frozen samples 1-2 m, frozen samples from 0-1 m and frozen samples from 1 to 2 m. This allowed us to calculate the mean C density for both depth increments for non-frozen and frozen samples, that were then used to calculate the C stocks for the top two meters of sediment deposits. For N, a depth decay model was not possible due to the lack of sufficient N data from greater sediment depths. Therefore, we split the N data in three parts, 0–1 m (non-frozen and frozen samples each), 1–2 m (non-frozen and frozen samples each), and >2 m (only includes frozen samples). For each of these parts we calculated the N density that was then used to calculate the N stocks for each depth increment.

Sediment volume and soil organic C and N calculations

In order to apply the depth decay derived C and N density values for each 1-m depth increment, we split the SV calculation in 1-meter depth increments as well (Supplementary Fig. S5.1). This allows us to apply the depth decay model in the C stock estimations. As a result, we calculated the C and N stock for each 1-m depth increment for each delta and in the final step summed these values to every delta's depth to derive the total soil organic C stored in each Arctic delta.

In order to respect the uncertainty in each input variable, we designed a model (Monte Carlo simulation) in the programming language R[82] that does not simply calculate C stock for each depth increment based on each input variables mean or median value. Our model randomly chooses a value that is between the lower and upper uncertainty range for each input variable (see Table 3) and for each delta. Then, the Monte Carlo simulation runs 10,000 times and calculates C stocks for each 1-m depth increment for every single delta 10,000 times. Also, the thickness of deposits varies in each of these 10,000 model runs for each delta according to the deltas 95% confidence interval depth range. In the end of each model run, the C (and N) stock for each delta is summed up to the respective depth which results in 10,000 variable depths of deposits and C stocks for each delta and each model run. In a final step, the C stock calculations for all the 211 deltas are summed together resulting in the total soil organic C

stored in Arctic river delta deposits. The 10,000 Monte Carlo simulation results are presented as a histogram (Fig. 3) illustrating the range of Arctic delta soil organic C stocks. From this distribution, we calculated the mean, as well as the 95% confidence intervals (2.5 and 97.5th percentiles). This Monte Carlo simulation propagates parametric uncertainty from the input variables in the soil organic C calculations.

Sensitivity analysis of the model

The model allows us to calculate the C and N stocks based on input variables that have an uncertainty assigned to it. In order to test for the sensitivity of the model to each input variable, we carried out a sensitivity analysis for every single input variable. We increased and decreased the investigated variable by 25% and checked how this affected the final result. The result of this sensitivity analyses show that the C stock is mainly driven by the C density, area of deltas, and the delta deposit thickness (see Supplementary Table S7.1). The other variables only have a minor impact (< 2%) on the final results. In a second sensitivity analysis, we let the model run again with all but one variable stable. The model was then run with selecting random values from the uncertainty range only for the tested variable. This allowed us to see the impact of each variable on the uncertainty estimation. This analysis shows that the deposit thickness has the largest effect on the uncertainty of the model, followed by the area (Supplementary Table S7.2). In fact, more than 60% of the model uncertainty is explained by the uncertainty in thickness of deposits. Area (19%) and C density (11%) are also responsible for large parts of the uncertainty while ice-wedge volume, permafrost distribution, and active layer depth only affect the uncertainty estimates in minor ways (Supplementary Table S7.2).

Non-deltaic deposits in the deltas

A special case for Arctic deltas is Arga Island in the Lena Delta, because it is characterized by late Pleistocene fluvial, alluvial sand deposits fragmented by thermokarst lakes[49]. Arga Island comprises 36% of the modern Lena Delta but is not part of the active delta anymore. We calculated the C and N stocks for these deposits (see supplementary chapter S8.1) in addition to the deltaic deposits. Arga Island was not included in the area estimate or stock calculations of the Lena Delta.

In addition, some of the mega and large deltas (e.g. Lena, Kolyma) include additional non-deltaic deposits such as Yedoma. Yedoma deposits are remnants of former late Pleistocene accumulation plains in Siberia, Alaska and Northwest Canada including Laptev and East Siberian Sea shelfs and are dissected by the fluvial processes in the Olenyok, Lena, and Kolyma deltas in North Siberia. Separate estimates for C based on source[50] and for N based on source[84] were completed for Yedoma deposits in deltas (information and data in Supplementary Material S8.2 and Table S8.1). Moreover, we excluded large, not delta-affected deposits (river does not flow through) that are elevated and not completely surrounded by the delta, such as Richards Island in the Mackenzie Delta[144]. Hence, they are not included in total C and N stock estimates.

Limitations and identification of gaps

Only 14% of the soil profiles are deeper than two meters, and therefore, the data set does not accurately represent deeper delta deposits. In addition, there are no samples available from deeper non-frozen deposits, which would lower the uncertainty of frozen and non-frozen C stock estimates. However, this is the best available data set to date. Previous pan-Arctic upscaling studies[2,10,50] faced an even stronger limitation of deep deposit data. We therefore implemented a depth-decay model for TOC so that we do not overestimate deep deposits. However, additional data from deeper soil layers, especially also from deep non-frozen deposits would be beneficial in order to have a better representation and lower the uncertainty in deep deltaic deposits. Nevertheless, near-surface sediments comprise sites across the entire alluvial succession and deeper deposits are likely reworked materials for these succession patterns. Therefore, we believe that we have a good representation of the different soil horizons. In addition, deltaic deposits are not formed in the same way as typical soil profiles because accumulation and fast incorporation of organic matter in deltas occurs by flooding, erosion, and redeposition in addition to regular soil forming processes leading to well-mixed deposits of reworked sediments. Previous studies[58] showed that even soil horizons below organic poor surface deposits can have a high total organic C and total N content due to the fact of rapid accumulation and slow organic matter decomposition in permafrost environments.

Beside additional soil samples, more information about the thickness of deposits from Arctic deltas is needed. Our thickness estimates are based on a relationship between size and thickness of deposits from five deltas only. With our sensitivity analysis we show that deposit thickness is responsible for more than 60% of the uncertainty associated with the C stock estimates (see Supplementary Table S7.2). Nevertheless, this first-order approximation of deposit thickness with size of the delta holds up for lower latitude deltas as well (see Supplementary Fig. S2.2). In addition, accurate water depth information from water bodies in deltas could help to better constrain the SV and determine the ratio between frozen and non-frozen deposits below water bodies. There is a high variability in size and depth of water bodies in Arctic deltas, but so far, we lack accurate information on pan-Arctic lake depths in deltas that would help determine whether the water bodies freeze to the bottom and maintain permafrost or have floating ice with sediments underneath remaining unfrozen throughout the year causing the formation of a talik.

With our manual mapping, we could not map all the Arctic micro-deltas and river mouth zones but a representative subsample. In particular, river mouths on remote Arctic islands such as Novaya Zemlya Island or small alluvial fans in Greenland were not mapped and thus not included. The effect of all the micro deltas on the final stock calculations is negligible as the mapped micro deltas only contribute 0.2% of the total delta area in the Arctic and contain about 0.1% of the C stored in Arctic delta deposits. Therefore, even by including 10 times as many micro deltas, the total Arctic delta C stock would change only by about 1%. However, we are confident that we mapped all the mega, large, medium, and small deltas present in the Arctic.

Data availability

New data: the data used for this study, including the resulting soil carbon and nitrogen stocks for each delta is available on the PANGAEA data set repository as a data set bundle (https://doi.org/10.1594/PANGAEA.967651)[145]. This data set splits into four different data sets: 1) the entire soil core and 2) sample data set including both the newly available and already published data sets. 3) The resulting data set with SV, soil organic C, soil N, water area coverage, deposit thickness, and area for every single delta, and 4) the geospatial layer (the product of the mapping) of river deltas will be available as a shapefile including an attribute table containing name, area, perimeter, and percentage water bodies. In addition, previously not published delta soil carbon and nitrogen data from North-West Alaskan deltas (https://doi.org/10.1594/PANGAEA.967493)[79] and the Lena delta (https://doi.org/10.1594/PANGAEA.967485)[80] are made available on PANGAEA.

Previously published soil organic C data sets used in this study are available on PANGAEA such as from the Lena Delta active floodplain and first unit (https://doi.org/10.1594/PANGAEA.728539[146]; https://doi.org/10.1594/PANGAEA.826958[147]; https://doi.org/10.1594/PANGAEA.862961[148]; https://doi.org/10.1594/PANGAEA.883582[149]; https://doi.org/10.1594/PANGAEA.959782[81]; https://doi.org/10.1594/PANGAEA.891142[150]) from Arga Island (https://doi.org/10.1594/PANGAEA.128931[151]; https://doi.org/10.1594/PANGAEA.611537[152]; https://doi.org/10.1594/PANGAEA.611530[153]; https://doi.org/10.1594/PANGAEA.

611538[154]); from the Kolyma Delta (https://doi.org/10.1594/PANGAEA.887933[155]); from the Ikpikpuk and Fish Creek Delta (https://doi.org/10.1594/PANGAEA.890883[156]); and data sets stored on the Bolin Center Database (https://bolin.su.se/data/) from the Zackenberg Delta (https://doi.org/10.17043/palmtag-2022-pedon-1[157,158]); and from previous delta C stock estimates (https://doi.org/10.5879/ecds/00000001[159]; https://doi.org/10.5194/essd-5-3-2013[160]) including data from the Mackenzie Delta.

Code availability

The depth decay model and the carbon and nitrogen stock calculations were performed in R, version 4.4.2. The R scripts for these analyses are available on Zenodo (https://doi.org/10.5281/zenodo.18530447).

References

1. Overeem, I., Nienhuis, J. H. & Piliouras, A. Ice-dominated Arctic deltas. *Nat. Rev. Earth Environ.* **3**, 225–240 (2022).
2. Tarnocai, C. et al. Soil organic carbon pools in the northern circumpolar permafrost region. *Glob. Biogeochem. Cycles* **23**, GB2023 (2009).
3. Mann, P. J. et al. Degrading permafrost river catchments and their impact on Arctic Ocean nearshore processes. *Ambio* **51**, 439–455 (2022).
4. Ogneva, O. et al. Particulate organic matter in the Lena River and its delta: from the permafrost catchment to the Arctic Ocean. *Biogeosciences* **20**, 1423–1441 (2023).
5. Walker, H. J. Arctic Deltas. *J. Coast. Res.* **14**, 719–738 (1998).
6. Jorgenson, M. T., Shur, Y. L. & Walker, H. J. Evolution of a permafrost-dominated landscape on the Colville River Delta, northern Alaska. In *Proceedings of the Seventh International Conference on Permafrost*, vol. 57, 523-529 (Collection Nord, 1998).
7. Lauzon, R., Piliouras, A. & Rowland, J. C. Ice and permafrost effects on delta morphology and channel dynamics. *Geophys. Res. Lett.* **46**, 6574–6582 (2019).
8. Schwamborn, G. et al. Fluvial and permafrost history of the lower Lena River, north-eastern Siberia, over late Quaternary time. *Sedimentology* **70**, 235–258 (2023).
9. Bolshiyanov, D., Makarov, A. & Savelieva, L. Lena River delta formation during the Holocene. *Biogeosciences* **12**, 579–593 (2015).
10. Hugelius, G. et al. Estimated stocks of circumpolar permafrost carbon with quantified uncertainty ranges and identified data gaps. *Biogeosciences* **11**, 6573–6593 (2014).
11. Rantanen, M. et al. The Arctic has warmed nearly four times faster than the globe since 1979. *Commun. Earth Environ.* **3**, 168 (2022).
12. AMAP. *Arctic Climate Change Update 2021: Key Trends and Impacts. Summary for Policy-Makers*. (Arctic Monitoring and Assessment Programme, 2021).
13. Jansen, E. et al. Past perspectives on the present era of abrupt Arctic climate change. *Nat. Clim. Chang.* **10**, 714–721 (2020).
14. Overeem, I. & Syvitski, J. P. M. Shifting discharge peaks in arctic rivers, 1977–2007. *Geografiska Annaler Ser. A, Phys. Geogr.* **92**, 285–296 (2010).
15. Blaskey, D. et al. Increasing Alaskan river discharge during the cold season is driven by recent warming. *Environ. Res. Lett.* **18**, 024042 (2023).
16. Feng, D. et al. Recent changes to Arctic river discharge. *Nat. Commun.* **12**, 6917 (2021).
17. Tank, S. E., Striegl, R. G., McClelland, J. W. & Kokelj, S. V. Multi-decadal increases in dissolved organic carbon and alkalinity flux from the Mackenzie drainage basin to the Arctic Ocean. *Environ. Res. Lett.* **11**, 054015 (2016).
18. Kokelj, S. V. et al. Thaw-driven mass wasting couples slopes with downstream systems, and effects propagate through Arctic drainage networks. *Cryosphere* **15**, 3059–3081 (2021).
19. Lesack, L. F. W., Marsh, P., Hicks, F. E. & Forbes, D. L. Local spring warming drives earlier river-ice breakup in a large Arctic delta. *Geophys. Res. Lett.* **41**, 1560–1567 (2014).
20. Rowland, J. C. et al. A morphology independent methodology for quantifying planview river change and characteristics from remotely sensed imagery. *Remote Sens. Environ.* **184**, 212–228 (2016).
21. Rowland, J. & Stauffer, S. Pan-arctic river bank erosion and accretion, and planform metrics measured over intervals ranging from 1973 to 2016. Environmental System Science Data Infrastructure for a Virtual Ecosystem; Incorporating the Hydrological Controls on Carbon Cycling in Floodplain Ecosystems into Earth System Models (ESMs). https://doi.org/10.15485/1571527 (2019).
22. Rowland, J. C. et al. Scale-dependent influence of permafrost on riverbank erosion rates. *JGR Earth Surf.* **128**, e2023JF007101 (2023).
23. Douglas, M. M. & Lamb, M. P. A model for thaw and erosion of permafrost riverbanks. *JGR Earth Surf.* **129**, e2023JF007452 (2024).
24. Ielpi, A., Lapôtre, M. G. A., Finotello, A. & Roy-Léveillée, P. Large sinuous rivers are slowing down in a warming Arctic. *Nat. Clim. Chang.* **13**, 375–381 (2023).
25. Biskaborn, B. K. et al. Permafrost is warming at a global scale. *Nat. Commun.* **10**, 264 (2019).
26. Stroeve, J. & Notz, D. Changing state of Arctic sea ice across all seasons. *Environ. Res. Lett.* **13**, 103001 (2018).
27. Irrgang, A. M. et al. Drivers, dynamics and impacts of changing Arctic coasts. *Nat. Rev. Earth Environ.* **3**, 39–54 (2022).
28. Box, J. E. et al. Global sea-level contribution from Arctic land ice: 1971–2017. *Environ. Res. Lett.* **13**, 125012 (2018).
29. Nienhuis, J. H. et al. River deltas and sea-level rise. *Annu. Rev. Earth Planet. Sci.* **51**, 79–104 (2023).
30. Vermaire, J. C. et al. Arctic climate warming and sea ice declines lead to increased storm surge activity. *Geophys. Res. Lett.* **40**, 1386–1390 (2013).
31. Zhang, Y. et al. The thermal response of permafrost to coastal floodplain flooding. *Environ. Res. Lett.* **18**, 035004 (2023).
32. Broaddus, C. M. et al. First-order river delta morphology is explained by the sediment flux balance from rivers, waves, and tides. *Geophys. Res. Lett.* **49**, e2022GL100355 (2022.).
33. Nill, L. et al. Arctic shrub expansion revealed by Landsat-derived multitemporal vegetation cover fractions in the Western Canadian Arctic. *Remote Sens. Environ.* **281**, 113228 (2022).
34. Tape, K. D., Jones, B. M., Arp, C. D., Nitze, I. & Grosse, G. Tundra be dammed: beaver colonization of the Arctic. *Glob. Change Biol.* **24**, 4478–4488 (2018).
35. Wenzel, G. W. Canadian Inuit subsistence and ecological instability—if the climate changes, must the Inuit? *Polar Res.* **28**, 89–99 (2009).
36. Bendixen, M. et al. Promises and perils of sand exploitation in Greenland. *Nat. Sustain* **2**, 98–104 (2019).
37. Kokelj, S. V., Riseborough, D., Coutts, R. & Kanigan, J. C. N. Permafrost and terrain conditions at northern drilling-mud sumps: Impacts of vegetation and climate change and the management implications. *Cold Reg. Sci. Technol.* **64**, 46–56 (2010).
38. Gill, R. E. & Handel, C. M. The importance of subarctic intertidal habitats to shorebirds: a study of the Central Yukon-Kuskokwim Delta, Alaska. *Condor* **92**, 709 (1990).
39. Lantz, T. C., Kokelj, S. V. & Fraser, R. H. Ecological recovery in an Arctic delta following widespread saline incursion. *Ecol. Appl.* **25**, 172–185 (2015).

40. Klein, D. R. Waterfowl in the economy of the eskimos on the Yukon-Kuskokwim Delta, Alaska. *Arctic* **19**, 319–336 (1966).
41. Nienhuis, J. H. et al. Global-scale human impact on delta morphology has led to net land area gain. *Nature* **577**, 514–518 (2020).
42. Galloway, W. E. Process framework for describing the morphologic and stratigraphic evolution of deltaic depositional systems. In *Deltas models for Exploration* (ed. Broussard, M. L.) 87–98 (Houston Geological Society, 1975).
43. Piliouras, A. & Rowland, J. C. Arctic river delta morphologic variability and implications for riverine fluxes to the coast. *J. Geophys. Res. Earth Surf.* **125**, 5250 (2020).
44. Kokelj, S. V. & Burn, C. R. Near-surface ground ice in sediments of the Mackenzie Delta, Northwest Territories, Canada. *Permafr. Periglac.* **16**, 291–303 (2005).
45. Korotayev, V. N. Geomorphology of river deltas on the arctic coast of Siberia. *Polar Geogr. Geol.* **10**, 139–147 (1986).
46. Strauss, J. et al. Organic-matter quality of deep permafrost carbon – a study from Arctic Siberia. *Biogeosciences* **12**, 2227–2245 (2015).
47. Tanski, G. et al. Rapid CO_2 release from eroding permafrost in seawater. *Geophys. Res. Lett.* **46**, 11244–11252 (2019).
48. Schuur, E. A. G. et al. Climate change and the permafrost carbon feedback. *Nature* **520**, 171–179 (2015).
49. Schwamborn, G., Rachold, V. & Grigoriev, M. N. Late Quaternary sedimentation history of the Lena Delta. *Quat. Int.* **89**, 119–134 (2002).
50. Strauss, J. et al. The deep permafrost carbon pool of the Yedoma region in Siberia and Alaska. *Geophys. Res. Lett.* **40**, 6165–6170 (2013).
51. Anthony, K. M. W. et al. A shift of thermokarst lakes from carbon sources to sinks during the Holocene epoch. *Nature* **511**, 452–456 (2014).
52. Olefeldt, D. et al. Circumpolar distribution and carbon storage of thermokarst landscapes. *Nat. Commun.* **7**, 13043 (2016).
53. Treat, C. C. et al. Widespread global peatland establishment and persistence over the last 130,000. *y. Proc. Natl. Acad. Sci. USA.* **116**, 4822–4827 (2019).
54. Hugelius, G. et al. Large stocks of peatland carbon and nitrogen are vulnerable to permafrost thaw. *Proc. Natl. Acad. Sci. USA.* **117**, 20438–20446 (2020).
55. Miesner, F. et al. Subsea permafrost organic carbon stocks are large and of dominantly low reactivity. *Sci. Rep.* **13**, 9425 (2023).
56. Lininger, K. B., Wohl, E., Rose, J. R. & Leisz, S. J. Significant floodplain soil organic carbon storage along a large high-latitude river and its tributaries. *Geophys. Res. Lett.* **46**, 2121–2129 (2019).
57. Palmtag, J., Cable, S., Christiansen, H. H., Hugelius, G. & Kuhry, P. Landform partitioning and estimates of deep storage of soil organic matter in Zackenberg, Greenland. *Cryosphere* **12**, 1735–1744 (2018).
58. Fuchs, M. et al. Sedimentary and geochemical characteristics of two small permafrost-dominated Arctic river deltas in northern Alaska. *Arktos* **4**, 1–18 (2018).
59. Shmelev, D. et al. Estimation and sensitivity of carbon storage in permafrost of North-Eastern Yakutia: Estimation and sensitivity of carbon storage. *Permafr. Periglac. Process.* **28**, 379–390 (2017).
60. Siewert, M. B., Hugelius, G., Heim, B. & Faucherre, S. Landscape controls and vertical variability of soil organic carbon storage in permafrost-affected soils of the Lena River Delta. *CATENA* **147**, 725–741 (2016).
61. Jackson, R. B. et al. The ecology of soil carbon: pools, vulnerabilities, and biotic and abiotic controls. *Annu. Rev. Ecol. Evol. Syst.* **48**, 419–445 (2017).
62. Holmes, R. M. et al. A circumpolar perspective on fluvial sediment flux to the Arctic ocean. *Glob. Biogeochem. Cycles* **16**, 45-1–45–14 (2002).
63. Dunn, F. E. et al. Projections of declining fluvial sediment delivery to major deltas worldwide in response to climate change and anthropogenic stress. *Environ. Res. Lett.* **14**, 084034 (2019).
64. Piliouras, A., Lauzon, R. & Rowland, J. C. Unraveling the combined effects of ice and permafrost on arctic delta morphodynamics. *J. Geophys. Res. Earth Surf.* **126**, 5706 (2021).
65. Vonk, J. E. et al. Spatial variations in geochemical characteristics of the modern Mackenzie Delta sedimentary system. *Geochimica et. Cosmochimica Acta* **171**, 100–120 (2015).
66. Obu, J. et al. Northern Hemisphere permafrost map based on TTOP modelling for 2000–2016 at 1 km2 scale. *Earth-Sci. Rev.* **193**, 299–316 (2019).
67. Kanigan, J. C. N., Burn, C. R. & Kokelj, S. V. Ground temperatures in permafrost south of treeline, Mackenzie Delta, Northwest Territories. *Permafr. Periglac.* **20**, 127–139 (2009).
68. Nguyen, T., Burn, C. R., King, D. J. & Smith, S. L. Estimating the extent of near-surface permafrost using remote sensing, Mackenzie Delta, Northwest Territories. *Permafr. Periglac.* **20**, 141–153 (2009).
69. Stephani, E., Drage, J., Miller, D., Jones, B. M. & Kanevskiy, M. Taliks, cryopegs, and permafrost dynamics related to channel migration, Colville River Delta, Alaska. *Permafr. Periglac.* **31**, 239–254 (2020).
70. Payne, C., Panda, S. & Prakash, A. Remote sensing of river erosion on the Colville River, North Slope Alaska. *Remote Sens.* **10**, 397 (2018).
71. Walker, J., Arnborg, L. & Peippo, J. Riverbank erosion in the Colville Delta, Alaska. *Geografiska Annaler: Ser. A, Phys. Geogr.* **69**, 61–70 (1987).
72. Vesakoski, J.-M. et al. Arctic Mackenzie Delta channel planform evolution during 1983-2013 utilising Landsat data and hydrological time series. *Hydrol. Process.* **31**, 3979–3995 (2017).
73. Tape, K. D., Verbyla, D. & Welker, J. M. Twentieth century erosion in Arctic Alaska foothills: The influence of shrubs, runoff, and permafrost. *J. Geophys. Res.* **116**, G04024 (2011).
74. Rearden, A. & Fienup-Riordan, A. *Erinaput Unguvaniartut: So Our Voices Will Live: Quinhagak History and Oral Traditions*. Calista Elders Council and the Alaska Native Language Center (University of Alaska Fairbanks, 2013).
75. Kanevskiy, M. et al. Ground ice in the upper permafrost of the Beaufort Sea coast of Alaska. *Cold Reg. Sci. Technol.* **85**, 56–70 (2013).
76. Ping, C.-L. et al. Soil carbon and material fluxes across the eroding Alaska Beaufort Sea coastline. *J. Geophys. Res.* **116**, G02004 (2011).
77. Pekel, J.-F., Cottam, A., Gorelick, N. & Belward, A. S. High-resolution mapping of global surface water and its long-term changes. *Nature* **540**, 418–422 (2016).
78. Zubrzycki, S., Kutzbach, L., Grosse, G., Desyatkin, A. & Pfeiffer, E.-M. Organic carbon and total nitrogen stocks in soils of the Lena River Delta. *Biogeosciences* **10**, 3507–3524 (2013).
79. Fuchs, M. et al. Permafrost soil organic carbon and soil nitrogen data from the Noatak, Kobuk and Selawik river deltas in Northwestern Alaska [dataset bundled publication]. PANGAEA https://doi.org/10.1594/PANGAEA.967493 (PANGAEA, 2026).
80. Fuchs, M., Strauss, J. & Grosse, G. Geochemical data for SOB14-A-21, a Lena Delta 1st terrace exposure. PANGAEA https://doi.org/10.1594/PANGAEA.967485 PANGAEA, (2024).
81. Treat, C. C., Fuchs, M. & Laurent, M. Below-ground carbon stocks and soil properties in the central Lena River Delta, Kurungnakh and Samoylov Islands from 12 permafrost profiles sampled in 2018.

3696 data points PANGAEA https://doi.org/10.1594/PANGAEA.959782 (PANGAEA, 2023).
82. R Core Team, R. R: a language and environment for statistical computing. (R Core Team, 2013).
83. Harden, J. W. et al. Field information links permafrost carbon to physical vulnerabilities of thawing. *Geophys. Res. Lett.* **39**, 051958 (2012).
84. Strauss, J. et al. A globally relevant stock of soil nitrogen in the Yedoma permafrost domain. *Nat. Commun.* **13**, 6074 (2022).
85. Juhls, B. et al. Serpentine (Floating) ice channels and their interaction with riverbed permafrost in the Lena River Delta, Russia. *Front. Earth Sci.* **9**, 689941 (2021).
86. Whitley, M. et al. Assessment of LiDAR and spectral techniques for high-resolution mapping of sporadic permafrost on the Yukon-Kuskokwim Delta, Alaska. *Remote Sens.* **10**, 258 (2018).
87. Pastick, N. J. et al. Spatial variability and landscape controls of near-surface permafrost within the Alaskan Yukon River Basin. *JGR Biogeosci.* **119**, 1244–1265 (2014).
88. Turetsky, M. R. et al. Carbon release through abrupt permafrost thaw. *Nat. Geosci.* **13**, 138–143 (2020).
89. Fuchs, M. et al. Rapid fluvio-thermal erosion of a Yedoma Permafrost Cliff in the Lena River Delta. *Front. Earth Sci.* **8**, 336 (2020).
90. Kanevskiy, M. et al. Patterns and rates of riverbank erosion involving ice-rich permafrost (yedoma) in northern Alaska. *Geomorphology* **253**, 370–384 (2016).
91. Laurent, M. et al. Relationships between greenhouse gas production and landscape position during short-term permafrost thaw under anaerobic conditions in the Lena Delta. *Biogeosciences* **20**, 2049–2064 (2023).
92. Herbst, T., Fuchs, M., Liebner, S. & Treat, C. C. Carbon stocks and potential greenhouse gas production of permafrost-affected active floodplains in the Lena River Delta. *JGR Biogeosci.* **129**, e2023JG007590 (2024).
93. Galera, L. D. A., Eckhardt, T., Beer, C., Pfeiffer, E. & Knoblauch, C. Ratio of in situ CO_2 to CH_4 production and its environmental controls in polygonal Tundra Soils of Samoylov Island, Northeastern Siberia. *JGR Biogeosci.* **128**, e2022JG006956 (2023).
94. Rößger, N., Sachs, T., Wille, C., Boike, J. & Kutzbach, L. Seasonal increase of methane emissions linked to warming in Siberian tundra. *Nat. Clim. Chang.* **12**, 1031–1036 (2022).
95. Kuhry, P. et al. Lability classification of soil organic matter in the northern permafrost region. *Biogeosciences* **17**, 361–379 (2020).
96. Shur, Y. L. & Jorgenson, M. T. Cryostructure development on the floodplain of the Colville River Delta, northern Alaska. *Proc. Seventh Int. Conf. Permafr.* **57**, 993–1000 (1998).
97. Gill, D. The point bar environment in the Mackenzie River Delta. *Can. J. Earth Sci.* **9**, 1382–1393 (1972).
98. Elbasiouny, H., Abowaly, M., Abu, A. A. & Gad, A. Spatial variation of soil carbon and nitrogen pools by using ordinary Kriging method in an area of north Nile Delta, Egypt. *CATENA* **113**, 70–78 (2014).
99. Yu, J. et al. Soil organic carbon storage changes in coastal wetlands of the modern Yellow River Delta from 2000 to 2009. *Biogeosciences* **9**, 2325–2331 (2012).
100. Holmquist, J. R. et al. Accuracy and precision of tidal wetland soil carbon mapping in the conterminous United States. *Sci. Rep.* **8**, 9478 (2018).
101. Nahlik, A. M. & Fennessy, M. S. Carbon storage in US wetlands. *Nat. Commun.* **7**, 13835 (2016).
102. Maxwell, T. L. et al. Global dataset of soil organic carbon in tidal marshes. *Sci. Data* **10**, 797 (2023).
103. Maxwell, T. L. et al. Soil carbon in the world's tidal marshes. *Nat. Commun.* **15**, 10265 (2024).
104. Chan, N.-H. et al. An Arctic delta reduced-complexity model and its reproduction of key geomorphological structures. *Earth Surf. Dynam.* **11**, 259–285 (2023).
105. Ensom, T. P., Burn, C. R. & Kokelj, S. V. Lake- and channel-bottom temperatures in the Mackenzie Delta, Northwest Territories. *Can. J. Earth Sci.* **49**, 963–978 (2012).
106. Kokelj, S. V., Lantz, T. C., Kanigan, J., Smith, S. L. & Coutts, R. Origin and polycyclic behaviour of tundra thaw slumps, Mackenzie Delta region, Northwest Territories, Canada. *Permafr. Periglac.* **20**, 173–184 (2009).
107. Lai, S. Y. J., Hsiao, Y. & Wu, F. Asymmetric effects of subaerial and subaqueous basement slopes on self-similar morphology of prograding deltas. *JGR Earth Surf.* **122**, 2506–2526 (2017).
108. Korus, J. T. & Fielding, C. R. Asymmetry in Holocene river deltas: patterns, controls, and stratigraphic effects. *Earth-Sci. Rev.* **150**, 219–242 (2015).
109. Strauss, J. et al. Deep Yedoma permafrost: a synthesis of depositional characteristics and carbon vulnerability. *Earth-Sci. Rev.* **172**, 75–86 (2017).
110. Ulrich, M., Grosse, G., Strauss, J. & Schirrmeister, L. Quantifying wedge-ice volumes in Yedoma and Thermokarst basin deposits: wedge-ice volume calculation in Yedoma and Thermokarst basin deposits. *Permafr. Periglac. Process.* **25**, 151–161 (2014).
111. Morse, P. D. & Burn, C. R. Field observations of syngenetic ice wedge polygons, outer Mackenzie Delta, western Arctic coast, Canada. *J. Geophys. Res. Earth Surf.* **118**, 1320–1332 (2013).
112. Kartoziia, A. Assessment of the ice wedge polygon current state by means of UAV imagery analysis (Samoylov Island, the Lena Delta). *Remote Sens.* **11**, 1627 (2019).
113. Morse, P. D., Burn, C. R. & Kokelj, S. V. Near-surface ground-ice distribution, Kendall Island Bird Sanctuary, western Arctic coast. *Can. Permafr. Periglac.* **20**, 155–171 (2009).
114. Jorgenson, M. T. et al. Role of ground ice dynamics and ecological feedbacks in recent ice wedge degradation and stabilization. *JGR Earth Surf.* **120**, 2280–2297 (2015).
115. Walter Anthony, K. M. et al. Decadal-scale hotspot methane ebullition within lakes following abrupt permafrost thaw. *Environ. Res. Lett.* **16**, 035010 (2021).
116. Stettner, S. et al. Monitoring inter- and intra-seasonal dynamics of rapidly degrading ice-rich permafrost riverbanks in the Lena Delta with TerraSAR-X time series. *Remote Sens.* **10**, 51 (2017).
117. Vulis, L. et al. Channel network control on seasonal lake area dynamics in Arctic Deltas. *Geophys. Res. Lett.* **47**, 086710 (2020).
118. Mueter, F. J. & Litzow, M. A. Sea ice retreat alters the biogeography of the Bering Sea continental shelf. *Ecol. Appl.* **18**, 309–320 (2008).
119. Jorgenson, M. T. et al. Interacting sea-level rise, sea-ice loss, storm flooding, erosion, and permafrost thaw threaten ecosystems, wildlife, and communities on the Yukon-Kuskokwim Delta. *Earth's. Future* **13**, e2025EF006015 (2025).
120. Kokelj, S. V. et al. Using multiple sources of knowledge to investigate northern environmental change: regional ecological impacts of a storm surge in the outer Mackenzie Delta, N.W.T. *Arctic* **65**, 257–272 (2012).
121. Terenzi, J., Jorgenson, M. T., Ely, C. R. & Giguère, N. Storm-surge flooding on the Yukon-Kuskokwim Delta, Alaska. *Arctic* **67**, 360–374 (2014).
122. Syvitski, J. P. M. Sediment discharge variability in Arctic rivers: implications for a warmer future. *Polar Res.* **21**, 323–330 (2002).
123. Frost, G. V., Bhatt, U. S., Macander, M. J., Hendricks, A. S. & Jorgenson, M. T. Is Alaska's Yukon–Kuskokwim delta greening or browning? resolving mixed signals of Tundra vegetation dynamics and drivers in the maritime Arctic. *Earth Interact.* **25**, 76–93 (2021).

124. Lantz, T. C., Marsh, P. & Kokelj, S. V. Recent shrub proliferation in the Mackenzie delta uplands and microclimatic implications. *Ecosystems* **16**, 47–59 (2013).
125. Abbott, B. W. et al. Biomass offsets little or none of permafrost carbon release from soils, streams, and wildfire: an expert assessment. *Environ. Res. Lett.* **11**, 034014 (2016).
126. Liljedahl, A. K., Timling, I., Frost, G. V. & Daanen, R. P. Arctic riparian shrub expansion indicates a shift from streams gaining water to those that lose flow. *Commun. Earth Environ.* **1**, 50 (2020).
127. St Jacques, J. & Sauchyn, D. J. Increasing winter baseflow and mean annual streamflow from possible permafrost thawing in the Northwest Territories, Canada. *Geophys. Res. Lett.* **36**, 2008GL035822 (2009).
128. Holmes, R. M. *NOAA Arctic Report Card 2021: River Discharge*. National Oceanic and Atmospheric Administration. https://doi.org/10.25923/ZEVF-AR65 (NOAA, 2021).
129. McClelland, J. W., Déry, S. J., Peterson, B. J., Holmes, R. M. & Wood, E. F. A pan-arctic evaluation of changes in river discharge during the latter half of the 20th century. *Geophys. Res. Lett.* **33**, L06715 (2006).
130. Holmes, R. M. et al. Climate Change Impacts on the Hydrology and Biogeochemistry of Arctic Rivers. In *Climatic Change and Global Warming of Inland Waters* (eds Goldman, C. R., Kumagai, M. & Robarts, R. D.) 1–26 (Wiley, 2012). https://doi.org/10.1002/9781118470596.ch1.
131. Rawlins, M. A. et al. Analysis of the Arctic system for freshwater cycle intensification: observations and expectations. *J. Clim.* **23**, 5715–5737 (2010).
132. Box, J. E. et al. Key indicators of Arctic climate change: 1971–2017. *Environ. Res. Lett.* **14**, 045010 (2019).
133. Shkolnik, I., Pavlova, T., Efimov, S. & Zhuravlev, S. Future changes in peak river flows across northern Eurasia as inferred from an ensemble of regional climate projections under the IPCC RCP8.5 scenario. *Clim. Dyn.* **50**, 215–230 (2018).
134. Nienhuis, J. H. & Van De Wal, R. S. W. Projections of global delta land loss from sea-level rise in the 21st century. *Geophys. Res. Lett.* **48**, e2021GL093368 (2021).
135. Jorgenson, M. T. et al. *An Ecological Land Survey for the Colville River Delta, Alaska, 1996*. (ABR, Inc., 1997).
136. Johnston, G. H. & Brown, R. J. E. Stratigraphy of the Mackenzie River Delta, Northwest Territories, Canada. *Geol. Soc. Am. Bull.* **76**, 103 (1965).
137. Taylor, A. E., Dallimore, S. R. & Judge, A. S. Late Quaternary history of the Mackenzie–Beaufort region, Arctic Canada, from modelling of permafrost temperatures. 2. The Mackenzie Delta–Tuktoyaktuk Coastlands. *Can. J. Earth Sci.* **33**, 62–71 (1996).
138. Gilbert, G. L., Cable, S., Thiel, C., Christiansen, H. H. & Elberling, B. Cryostratigraphy, sedimentology, and the late Quaternary evolution of the Zackenberg River delta, northeast Greenland. *Cryosphere* **11**, 1265–1282 (2017).
139. Schwamborn, G., Rachold, V., Schneider, W., Grigoriev, M. N. & Nixdorf, U. Ground penetrating radar and shallow seismic-stratigraphic and permafrost investigations of Lake Nikolay, Delta Lena, Arctic Siberia. In *Proc. SPIE 4084, Eighth International Conference on Ground Penetrating Radar*, 783–789 (SPIE, 2000). https://doi.org/10.1117/12.383516.
140. Bode, J. A., Moorman, B. J., Stevens, C. W. & Solomon, S. M. Estimation of ice wedge volume in the Big Lake area, Mackenzie Delta, NWT, Canada. In *Proc. Ninth International Conference on Permafrost, Fairbanks, Alaska*, vol. 28 131–136 (Wiley, 2008).
141. Fritz, M. et al. Dissolved organic carbon (DOC) in Arctic ground ice. *Cryosphere* **9**, 737–752 (2015).
142. Williams, P. J. Ice distribution in permafrost profiles. *Can. J. Earth Sci.* **5**, 1381–1386 (1968).
143. Burn, C. R. & Kokelj, S. V. The environment and permafrost of the Mackenzie Delta area. *Permafr. Periglac.* **20**, 83–105 (2009).
144. Murton, J. B. Stratigraphy and palaeoenvironments of Richards Island and the eastern Beaufort Continental Shelf during the last glacial-interglacial cycle. *Permafr. Periglac.* **20**, 107–125 (2009).
145. Fuchs, M. et al. Arctic river delta soil and geospatial data set [dataset]. PANGAEA https://doi.org/10.1594/PANGAEA.967651 (2026).
146. Schwamborn, G., Rachold, V. & Grigoriev M. N. Sedimentation and mineral analysis on sediment cores from the Lena Delta, supplement to: Schwamborn, Georg; Rachold, Volker; Grigoriev, Mikhail N (2002): late quaternary sedimentation history of the Lena Delta. *Quat. Int.* **89**, 119–134 (2002).
147. Zubrzycki, S., Kutzbach, L., Grosse, G., Desyatkin, A. & Pfeiffer, E.-M. Organic carbon and total nitrogen stocks in soils of the Lena River Delta, supplement to: Zubrzycki, S.; Kutzbach, L.; Grosse, G.; Desyatkin, A.; Pfeiffer, E.-M. (2013): Organic carbon and total nitrogen stocks in soils of the Lena River Delta. *Biogeosciences* **10**, 3507–3524 (2013) https://doi.org/10.1594/PANGAEA.826958.
148. Siewert, et al. Soil organic carbon storage and soil properties for 50 soil profiles in the Lena River Delta including land form description and map, supplement to: Siewert, M. B.; Hugelius, G.; Heim, B.; Faucherre, S. (2016): Landscape controls and vertical variability of soil organic carbon storage in permafrost-affected soils of the Lena River Delta. *CATENA* **147**, 725–741 (2016) https://doi.org/10.1594/PANGAEA.862961.
149. Fuchs, M. et al. Sample site characteristics including mean SOC and SN for permafrost cores collected on Sobo-Sise Island and Bykovsky Peninsula, supplement to: Fuchs, M.; Grosse, G.; Strauss, J.; Günther, F.; Grigoriev, M. N.; Maximov, G. M.; Hugelius, G. (2018): carbon and nitrogen pools in thermokarst-affected permafrost landscapes in Arctic Siberia. *Biogeosciences* **15**, 953–971 (2017).
150. Boike, J. et al. Measurements in soil and air at Samoylov Station (2002–2018). 5 datasets (PANGAEA, 2018) https://doi.org/10.1594/PANGAEA.891142.
151. Schwamborn, G., Rachold, V. & Grigoriev, M. N. Age determinations and sedimentology Arga Island, Lena Delta. 39 data points PANGAEA https://doi.org/10.1594/PANGAEA.128931 (PANGAEA, 2002).
152. Schirrmeister, L. Lithology, colour and structural description of sediment profile T021, Appendix 4–2. 52 data points PANGAEA https://doi.org/10.1594/PANGAEA.611537 (PANGAEA, 2007).
153. Schirrmeister, L. Lithology, colour and structural description of sediment profile Ebe–2, Appendix 4-2. 28 data points PANGAEA https://doi.org/10.1594/PANGAEA.611530 (PANGAEA, 2007).
154. Schirrmeister, L. Lithology, colour and structural description of sediment profile Tur-1, Appendix 4-2. 125 data points PANGAEA https://doi.org/10.1594/PANGAEA.611538 (PANGAEA, 2007).
155. Schirrmeister, et al. Sediment, ground ice, geochronological and paleoecological data from polygon cores in the Siberian Arctic. 12 datasets (PANGAEA, 2018) https://doi.org/10.1594/PANGAEA.887933.
156. Fuchs, M. et al. Carbon, nitrogen and radiocarbon data from permafrost cores of two small Arctic river deltas in northern Alaska, supplement to: Fuchs, M.; Grosse, G.; Jones, B. M.; Strauss, J.; Baughman, C. A.; Walker, D. A. (2018): Sedimentary and geochemical characteristics of two small permafrost-dominated Arctic river deltas in northern Alaska. arktos - The Journal of Arctic Geosciences, 4. 3 datasets (PANGAEA, 2018) https://doi.org/10.1594/PANGAEA.890883.
157. Palmtag, J. et al. A high spatial resolution soil carbon and nitrogen dataset for the northern permafrost region based on circumpolar land cover upscaling. *Earth Syst. Sci. Data* **14**, 4095–4110 (2022).

158. Palmtag, Juri et al. Detailed pedon data on soil carbon and nitrogen for the northern permafrost region. Bolin Centre Database https://doi.org/10.17043/PALMTAG-2022-PEDON-1.
159. Bolin Centre For Climate Research. Archived data from Northern Circumpolar Soil Carbon DatabaseArchived data from Northern Circumpolar Soil Carbon Database. 385.92 MiB [object Object] https://doi.org/10.5879/ECDS/00000001 (ECDS, 2018).
160. Hugelius, G. et al. The Northern Circumpolar Soil Carbon Database: spatially distributed datasets of soil coverage and soil carbon storage in the northern permafrost regions. *Earth Syst. Sci. Data* **5**, 3–13 (2013).
161. Earth Resources Observation and Science (EROS) Center. *Landsat 8-9 Operational Land Imager / Thermal Infrared Sensor Level-2, Collection 2* U.S. Geological Survey. https://doi.org/10.5066/P9OGBGM6 (EROS, 2020).
162. Overduin, P. P. et al. Submarine permafrost map in the Arctic modeled using 1-D transient heat flux (SuPerMAP). *J. Geophys. Res. Oceans* **124**, 3490–3507 (2019).

Acknowledgements

This work is embedded into the Permafrost Carbon Network. We thank Michail Grigoriev for supporting field logistics in the Lena Delta, and Paul Göckeritz, Tanja Herbst and Dyke Scheidemann for their help with the laboratory analyses. We kindly acknowledge the support by the Research Station Samoylov Island and the Teshekpuk Lake Observatory for providing critical field logistics. In addition, we thank the U.S. Fish and Wildlife Service in Kotzebue, NANA Regional Cooperation, and the U.S. National Park Service for their support and their permissions granted for the field work in summer 2016 in northwest Alaska. This study was supported by the NERC-BMBF CACOON project (#03F0806A), ERC Starting Grant PETA-CARB (#338335), the Initiative and Networking Fund of the Helmholtz Association (#ERC-0013), the EU Nunataryuk project (#773421), the BMBF KoPf project (#03F0764B), the DFG project POLYGON (#164232461), ESA GlobPermafrost, Schmidt Sciences (PeTCaT project), and the U.S. National Science Foundation awards NSF #1927872, NSF #2052107, OISE-1927553, OPP-1903735, and OPP-2336164. The authors acknowledge support by the Open Access publication fund of Alfred-Wegener-Institut Helmholtz-Zentrum für Polar- und Meeresforschung.

Author contributions

M.F. and G.G. designed the idea of the study. M.F. led the data synthesis of published soil cores, mapped the deltas, carried out the calculations, and wrote the first manuscript draft with input from T.S., G.G. and J.S. M.F., G.H., B.M.J., L.K., I.N., J.P., C.L.P., E.R., L.S., G.S., M.B.S., J.S., A.R., A.V., S.Z. and G.G. collected or contributed sample data. I.N. provided input on the water mask and delta classification. M.F., L.L.J., G.H., G.V.F., B.M.J., I.N., J.P., C.L.P., S.V.K., P.P.O., O.S.P., L.S., M.B.S., J.S., C.T. and G.G. contributed to the analysis and interpretation of the data. All authors were involved in the writing and presentation of the data.

Competing interests

The authors declare no competing interests.

Additional information

Supplementary information The online version contains supplementary material available at https://doi.org/10.1038/s41467-026-73092-2.

Correspondence and requests for materials should be addressed to Matthias Fuchs.

Peer review information *Nature Communications* thanks Yating Chen and Jennifer A. Rogers for their contribution to the peer review of this work. A peer review file is available.

Reprints and permissions information is available at http://www.nature.com/reprints

Publisher's note Springer Nature remains neutral with regard to jurisdictional claims in published maps and institutional affiliations.

Open Access This article is licensed under a Creative Commons Attribution-NonCommercial-NoDerivatives 4.0 International License, which permits any non-commercial use, sharing, distribution and reproduction in any medium or format, as long as you give appropriate credit to the original author(s) and the source, provide a link to the Creative Commons licence, and indicate if you modified the licensed material. You do not have permission under this licence to share adapted material derived from this article or parts of it. The images or other third party material in this article are included in the article's Creative Commons licence, unless indicated otherwise in a credit line to the material. If material is not included in the article's Creative Commons licence and your intended use is not permitted by statutory regulation or exceeds the permitted use, you will need to obtain permission directly from the copyright holder. To view a copy of this licence, visit http://creativecommons.org/licenses/by-nc-nd/4.0/.

© The Author(s) 2026